Master's thesis

Denitrification and dissimilatory nitrate reduction to ammonium in a lake receiving wastewater effluent

Miikka Hasari

University of Jyväskylä

Department of Biological and Environmental Science

International Aquatic Masters Programme

February 2015

University of Jyväskylä, Faculty of Science

Department of Biological and Environmental Science
International Aquatic Masters Programme

Hasari Miikka: Denitrification and dissimilatory nitrate reduction to ammonium in a lake receiving wastewater effluent
Master's thesis: **40** p. + appendices 9 p.
Supervisors: Prof. Marja Tiirola, Dr. Antti Rissanen
Reviewers: Dr. Hannu Nykänen, Dr. Antti Rissanen
February 2015

Keywords: boreal lake, denitrification, DNRA, isotope pairing technique, wastewater effluent

ABSTRACT

Denitrification and dissimilatory nitrate reduction to ammonium (DNRA) are anoxic microbial nitrate-reducing processes, which occur for example in lake sediment and hypolimnion. Denitrification produces N_2 gas, which exits the water body, while DNRA produces ammonium, which is retained in the water. Wastewater effluent in a lake can be further purified by natural denitrification, but the role of DNRA is less known. Understanding these processes can help to improve wastewater treatment. In this thesis, rates of denitrification and DNRA and their correlations with water quality were studied in Lake Keurusselkä, where a wastewater treatment plant releases its effluent waters. Incubation and reactor experiments were conducted by using ^{15}N tracers.

The hypotheses were that the rates of denitrification are higher when wastewater effluent is present, and that the DNRA:denitrification ratio is also higher in the same conditions. The denitrification rates were highest near the effluent pipe, and in overall higher than those of DNRA. The ratio showed no such trend. Denitrification correlated positively with nitrate concentration and negatively with oxygen concentration and pH, while DNRA showed negative correlation with pH. The reactor experiment results showed initial positive correlation between ambient NO_3^- levels and denitrification, but not anymore after 24 hours of incubation.

JYVÄSKYLÄN YLIOPISTO, Matemaattis-luonnontieteellinen tiedekunta

Bio- ja ympäristötieteiden laitos
Akvaattiset tieteet

Hasari Miikka:	Denitrifikaatio ja DNRA (dissimilatory nitrate reduction to ammonium) järvessä joka vastaanottaa jätevedenpuhdistamon poistovettä
Pro gradu:	**40** s. + liiteet 9 s.
Työn ohjaajat:	Prof. Marja Tiirola, FT Antti Rissanen
Tarkastajat:	FT Hannu Nykänen, FT Antti Rissanen
Tammikuu 2015	

Hakusanat: boreaalinen järvi, denitrifikaatio, DNRA, isotooppileimaus, jätevedenpuhdistamon poistovesi

TIIVISTELMÄ

Denitrifikaatio ja DNRA (dissimilatory nitrate reduction to ammonium) ovat nitraattia pelkistäviä prosesseja, jotka yleensä esiintyvät hapettomissa olosuhteissa, kuten järvien sedimenteissä ja alusvesissä. Denitrifikaatiossa syntyy typpikaasua, joka poistuu ilmakehään, kun taas DNRA:n lopputuote on ammonium, joka jää veteen. Luonnollinen denitrifikaatio voi poistaa typpeä jätevedenpuhdistamon poistovedestä, mutta DNRA:n rooli on vähemmän tunnettu. Näiden prosessien tutkiminen voi auttaa jätevedenpuhdistuksen kehittämisessä. Tässä Pro Gradu –työssä tutkittiin denitrifikaation ja DNRA:n prosessinopeuksia sekä nopeuksien korrelaatioita erilaisten vedenlaatumuuttujien kanssa. Tutkimuspaikkana oli Keurusselkä –järvi, jonne paikallinen jätevedenpuhdistamo laskee poistovetensä. Metodina käytettiin isotooppileimausta inkubaatio- ja reaktorikokeissa.
Järvestä valittiin kolme näytteenottopistettä, joista kaksi sijaitsivat poistovesiputkesta myötävirtaan ja yhtä käytettiin kontrollina. Hypoteeseinä olivat: a) denitrifikaationopeudet ovat suurempia purkuputken läheisyydessä korkeamman nitraattipitoisuuden vuoksi, sekä b) DNRA:denitrifikaatio –suhde on niin ikään suurempi samoissa olosuhteissa. Denitrifikaationopeudet olivat korkeimmillaan purkuputken kohdalla ja ylipäätään suurempia kuin DNRA:n nopeudet. DNRA:denitrifikaatio –suhteessa ei havaittu merkittäviä eroja näytepisteiden tai ajankohtien välillä. Denitrifikaatio korreloi positiivisesti nitraattipitoisuuden kanssa ja negatiivisesti happipitoisuuden sekä pH:n kanssa. DNRA korreloi negatiivisesti pH:n kanssa. Reaktorikokeissa havaittiin aluksi positiivinen korrelaatio denitrifikaation ja veden nitraattipitoisuuden välillä, mutta 24 tunnin inkubaation jälkeen vastaavaa korrelaatiota ei enää esiintynyt.

Contents

1. INTRODUCTION

Anthropogenic nutrient loading into aquatic systems can lead to severe eutrophication, which poses threats to aquatic life, drinking-water supply and recreational use of the water bodies. In most aquatic ecosystems, the limiting nutrient for plant growth is either nitrogen (N) or phosphorous (P), or both. In the Baltic Sea, N has been recognized as the key limiting nutrient for spring phytoplankton production and the main factor sustaining the hypoxia in the bottom layer (Conley *et al.* 2009). Naturally occurring processes such as denitrification can be essential in removing N from water bodies. Studies have shown that most of the riverine nitrate (NO_3^-) entering Baltic Sea can be removed by the coastal system itself (Voss *et al.* 2011). Removing N already in inland aquatic systems is important, since N in lakes and rivers will eventually end up in the vulnerable coastal areas. Model-based estimations have suggested that lakes and reservoirs remove nearly one third of the N entering freshwater systems globally (Harrison *et al.* 2009).

Both municipal and industrial wastewater treatment can utilize microbial activity. The paired nitrification-denitrification process can be integrated into the activated sludge treatment and these solutions are already applied in Finland (Rissanen 2012). Denitrification can purify the effluent further after it has undergone treatment processes at the wastewater treatment plant (WWTP), as was shown in a study on Swedish wetlands (Andersson *et al.* 2005). The fate of wastewater effluent N in boreal lakes has not been previously studied, but the spatial allocation of NO_3^- could play an important role, i.e. whether the effluent is released into the bottom layer of the lake, where denitrification activity is high (Herbert 1999). Denitrification, which converts NO_3^- to nitrogen gas (N_2) under anoxic conditions, is one of the several microbial processes in the aquatic nitrogen cycle (Figure 1). Other processes in the cycle, such as dissimilatory nitrate reduction to ammonium (DNRA), can retain N in the system and inhibit the purification. The concentration of NO_3^- is considered the main factor limiting denitrification in boreal lakes (Rissanen *et al.* 2013). High salinity and high organic matter content are factors enhancing DNRA (Song *et al.* 2014). However, in tropical estuaries, high NO_3^- concentrations together with low organic matter content can result in DNRA outperforming denitrification (Dong *et al.* 2011). Sewage input with high N concentration can enhance N_2 production in an aquatic system (Zhao *et al.* 2014), and a constructed wetland can be efficient in removing N from the effluent (Abe *et al.* 2014).

The benthic zone of a lake that receives wastewater effluent can be considered an ideal location for studying denitrification because of the high NO_3^- content and lack of oxygen (O_2). The role of DNRA in such conditions is less known. Studies could help to improve the effectiveness of wastewater treatment. In this thesis, denitrification and DNRA rates were studied in Lake Keurusselkä, where a local WWTP releases its effluent waters, by utilizing stable isotope analysis (SIA) and isotope pairing technique (IPT) in incubation experiments. *In situ* measurements were done with benthic flux chambers, but these results (as well as N_2O production) will be presented in another Master's thesis. Additionally, two reactor experiments were conducted to study variations in denitrification and DNRA rates within different dilutions of wastewater. The hypotheses of the thesis are that a) denitrification rates in a boreal lake are higher when wastewater effluent with high NO_3^- concentration is present, and that b) the DNRA:Den ratio is higher in the same conditions.

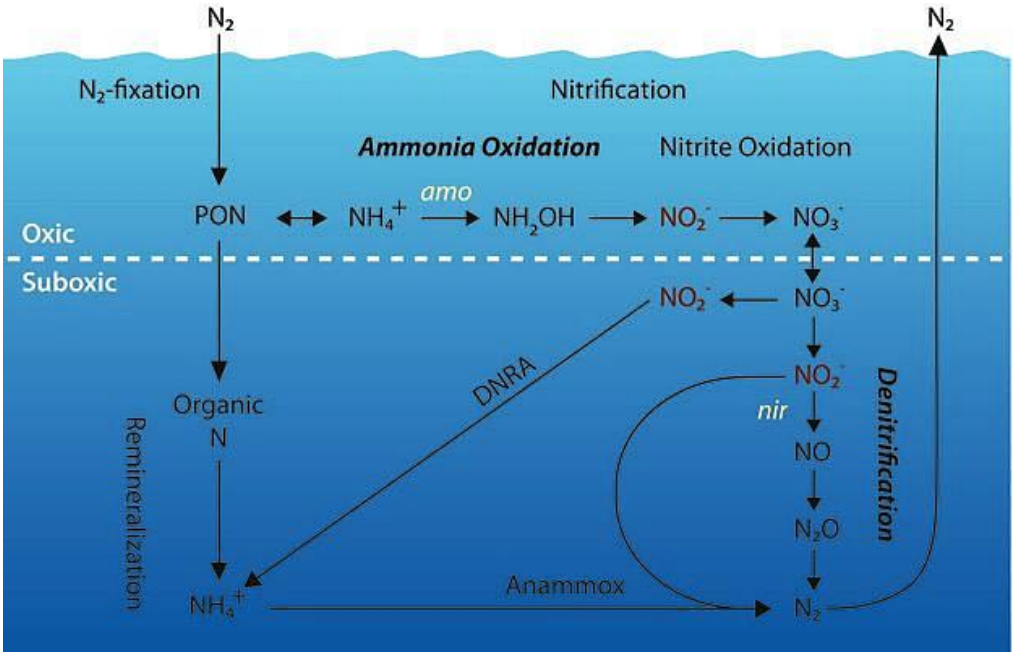

Figure 1. Nitrogen cycling in aquatic environments (modified from Francis *et al.* 2007 by Francis 2012).

2. BACKGROUND

2.1 Sources and sinks of nitrogen

Anthropogenic activities contribute significantly to the amount of bioavailable N. Fertilizer production involves industrial N fixation and crops with symbiotic N-fixing microbes are cultivated (Vitousek *et al.* 1997). The burning of fossil fuels releases nitrogen oxides (NO_x) into the atmosphere (Jaeglé *et al.* 2005). Rock weathering, volcanic activity and atmospheric fixation via ionizing radiation and electrical discharge also contribute to the amount of N at the surface of the earth (Canfield *et al.* 2005).

Many prokaryotes are capable of N fixation, a process that transforms gaseous nitrogen in the atmosphere to biologically available ammonia (NH_3). The process involves breaking the triple bond of N_2, which requires a significant amount of energy. Therefore it takes place only in certain environments and conditions, and only by certain organisms with the nitrogenase enzyme. N fixation does not take place if there is already fixed N available (Kirchman 2012). Combined N from planktonic fixation, catchment area loading and atmospheric deposition can lead to eutrophication in water bodies (Conley *et al.* 2009, Bergström *et al.* 2006, Schindler 2006). However, inland surface waters can act as important N sinks due to the many possible fates of N once it enters these systems (Harrison *et al.* 2009).

N undergoes various transformation processes in aquatic environments (Figure 1). N is removed from the system by processes that convert N compounds to gases which dissipate into the atmosphere. These include the anaerobic ammonium oxidation (Anammox), which converts ammonium (NH_4^+) and nitrite (NO_2^-) to N_2, as well as the denitrification process, which reduces NO_3^- to N_2 (Kirchman 2012). N retaining processes include dissimilatory

nitrate reduction to ammonium (DNRA). Another source of NH_4^+ is ammonification, which turns the N compounds of organic matter into NH_4^+ as the heterotrophic organisms break down prokaryote cells. (Canfield *et al.* 2005).

2.2 Denitrification and DNRA

Denitrification is a multi-stage process of NO_3^- reduction carried out by various bacteria, archaea and fungi. The microbes that are capable of carrying out denitrification include several subclasses of the Proteobacteria group, as well as halophilic and hyperthermophilic archaea. The process is called heterotrophic denitrification if organic matter is oxidized and autotrophic denitrification when oxidation of inorganic matter such as hydrogen and reduced sulphur or iron compounds takes place. (Zumft 1997).

Denitrification usually takes place under O_2 depletion which can lead to bacteria respiring NO_x as substitute terminal electron acceptors. A common environment for denitrification is in the sediments of aquatic systems where anoxic conditions are present (Herbert 1999). Most of the denitrifying microbes also respire O_2 and there are no known bacteria that only use denitrification when producing ATP (Shapleigh 2013).

There are four reductase enzymes involved in the complete denitrification pathway; nitrate reductase (nar), nitrite reductase (nir), nitric oxide reductase (nor) and nitrous oxide reductase (nos). The NADH dehydrogenase acts as a reducing agent and donates electrons to the reductases involved (Chen & Strous 2013). The complete denitrification pathway consists of NO_3^- being reduced to a gas with the intermediate forms of NO_2^-, nitric oxide (NO) and nitrous oxide (N_2O) (Francis *et al.* 2007). However, some denitrifying microbes lack one or more of the necessary enzymes for the complete pathway and in these cases some of the intermediary steps are omitted (Canfield *et al.* 2005). An alternative process to denitrification is DNRA, in which the NO_3^- is transformed to nitrite (NO_2^-) and then to ammonium (NH_4^+), thus retaining the N in the water body. The process utilizes NO_3^- and NO_2^- as electron acceptors and it can be carried out by various anaerobic bacteria with the nitrite reductase (nrfA) enzyme (Simon 2002).

Nutrient content, temperature and pH are among the properties of a water body that affect the rates of denitrification and DNRA. One of the key factors is carbon to total nitrogen (C/N) ratio. Laboratory-scale sequencing batch biofilm reactor operating at three different C/N ratios showed that a lower ratio results in lower N removal, most likely due to the lack of organic carbon which could be used as electron donor. However, too much organic carbon inhibited the nitrifying bacteria growth. The results also concurred with some previous studies about the optimal C/N ratio for denitrification being around 10:1 to 11:1. (Tan *et al.* 2013). The C/N ratio in combination with microbial generation time and the supply of NO_2^- and NO_3^- was seen as the key factor controlling denitrification and DNRA by Kraft *et al.* (2014); denitrification prevailed with carbon limitation, excess of both NO_2^- and NO_3^-, and with shorter generation times. High C/N ratio coupled with high salinity can enhance DNRA (Carrey *et al.* 2014).

The denitrification rates are also linked with the availability of NO_3^-; higher rates occur with higher NO_3^- content (Rissanen *et al.* 2013) and the supply of NO_3^- is indeed considered the most important factor controlling denitrification (McCrackin & Elser 2010). DNRA requires less NO_3^- than denitrification and it is used to detoxify NO_2^-. Sometimes it can also

act as an electron sink for fermentation (Canfield *et al.* 2005). High sulfide concentrations might contribute to higher DNRA rates (Behrendt *et al.* 2013), which could even exceed those of denitrification (Mazéas *et al.* 2008). A Polish study showed a positive correlation of temperature and organic matter content with DNRA rates (Tomaszek & Gruca-Rokosz 2007).

Declining pH was one of the factors that lead to higher denitrification rates in a Finnish lake (Rissanen *et al.* 2011). A study has shown that the optimal influent pH for maximum denitrification in a wastewater purification system is around 6.0-7.0, while more basic water strongly inhibits the gas formation; the denitrification completely stopped at pH 9.0 (Song *et al.* 2013). Another study on a sequencing batch reactor indicated that highest NO_3^- reduction took place at pH 7.0, while NO_2^- reduction was most efficient at pH 7.5 (Pan *et al.* 2012). The same study noted that the N_2O reduction rate was more sensitive to changes in acidity than the other reduction processes; lower pH yielded lower N_2O reduction rates.

In addition to pH, temperature can be another important variable. If the system or reactor is warm, more NO_3^- can be removed compared to cold conditions (Warneke *et al.* 2011). A more precise evaluation was provided in another study by Misiti *et al.* (2011), in which denitrification rates were measured in temperatures of 5, 10, 15 and 22 °C. There was little difference between the two higher temperatures, but the colder conditions yielded much less efficient NO_3^- removal rates. However, complete denitrification was achieved even in 5 °C, due to adequate amount of dissolved biodegradable carbon. Flow-through reactor experiments indicate that denitrification has seasonal variation, with higher rates observed during summertime temperatures (Laverman *et al.* 2007), and *in situ* experiments have shown similar results (Merchán *et al.* 2014). Tropical temperatures together with low organic matter contents and high NO_3^- concentrations can provide conditions that are more favorable to DNRA, as suggested by a study on three tropical estuaries (Dong *et al.* 2011). However, the observations by Nizzoli *et al.* (2010) indicate that lakes which are rich in organic matter and NO_3^- might favor DNRA over denitrification during summer stratification. Another estuarine study showed that DNRA bacteria dominate during warm temperatures, while denitrifiers are more active during colder periods (Ogilvie *et al.* 1997). In boreal lakes the denitrification rates can become higher as the temperature decreases, while NH_4^+ concentrations can increase along with temperature (Rissanen *et al.* 2011).

The boreal region contains many lakes and there has been some previous studies of denitrification in that area (Table 1), including measurements in Finnish lakes Lehee, Suolijärvi, Pääjärvi (Rissanen *et al.* 2013), Ormajärvi (Rissanen *et al.* 2011) and Kirkkojärvi (Holmroos *et al.* 2012) as well as Swedish lakes Vallentuna and Norrviken (Ahlgren *et al.* 1994). Boreal lake DNRA has not been previously studied.

Table 1. Mean denitrification rates and additional information of seven boreal lakes (modified from Rissanen *et al.* 2013). 1: Lehee; 2: Suolijärvi; 3: Ormajärvi; 4: Pääjärvi; 5: Kirkkojärvi; 6: Vallentuna; 7: Norrviken.; n: number of observations; NO_3^-, O_2 and *T*: nitrate concentrations, oxygen concentrations and temperatures of the water overlying the sediment; Den: denitrification; D_n: coupled nitrification-denitrification; D_w: denitrification of the nitrate in the water overlying the sediment; SD: standard deviation.

Lake (n)	NO_3^- (µmol l^{-1})	SD	O_2 (µmol l^{-1})	SD	*T* (°C)	SD	Den (µmol N m^{-2} d^{-1})	SD	D_n (µmol N m^{-2} d^{-1})	SD	D_w (µmol N m^{-2} d^{-1})	SD
1 (2)	2.2	0.6	290.6	39.8	14.7	4.1	53.8	12.7	29.1	2.4	24.7	15.1
2 (2)	15.8	2.8	185.9	174.6	10.7	1.1	215.9	0.2	64.5	25.6	151.4	25.4
3 (12)	19.7	14.1	328.6	69.4	10.9	6.8	220.2	119.7	112.5	53.9	107.7	99.9
4 (2)	64.3	0.5	328.1	17.7	11.2	0.8	269.2	12.3	183.6	6.0	85.6	6.3
5 (3)	30.0	26.1	310.4	65.7	11.1	9.9	282.6	114.6	140.2	81.2	142.4	127.3
6 (20)	6.3	6.2	305.9	99.1	8.8	6.2	57.0	23.7	28.1	28.3	28.9	34.4
7 (9)	9.5	11.1	336.4	88.5	8.5	5.7	53.9	46.0	35.3	53.7	18.6	23.1

2.3 Stable isotope analysis

Isotopes are variations of elements differing in their number of neutrons. Extra neutrons increase the mass of the element, but chemically two different isotopes behave in a fairly similar manner. Stable isotopes do not decay or pose health risks, and they can be essential in studying the cycling of elements. N has two stable isotopes, the lighter ^{14}N and the heavier ^{15}N. The ^{14}N is far more abundant in nature as it accounts for over 99.6% of N_2 in the air. (Hayes 2002).

Isotope fractionation causes differences in the ratios of isotopes. This is the effect of the extra neutron in the heavier isotope, which causes subtle variation in the reaction rates. In kinetic reactions the lighter isotopes usually react faster because less energy is required. For example, the uptake of N by phytoplankton causes fractionation in aquatic systems, but to a lesser extent when N is the limiting nutrient. The effects of fractionation are predictable in various systems, and they must be taken into account when studying reactions like denitrification with the help of natural stable isotopic ratio of N. (Fry 2006).

One method for measuring N_2 gas production is using ^{15}N tracers. Both fractionation and the natural occurrence of the heavier isotope can be neglected when using an adequate amount of the tracer (Rissanen 2012). Commercially produced tracers are added to samples which are then left to incubate. The amounts of ^{15}N-labeled N_2 gas and NH_4^+ produced during the incubation can be measured with an isotope-ratio mass spectrometer (IRMS). The natural denitrification rate is estimated from the ^{15}N-labeled gas production. The ^{15}N labeling of NO_3^- that is reduced to NH_4 equals the ^{15}N labeling of nitrate used for denitrification, and thus the natural DNRA can be estimated from ^{15}N-labeled NH_4 production. (Nielsen 1992, Christensen *et al.* 2000).

IPT can be used to determine rates of natural denitrification (D_{14}), coupled nitrification-denitrification (D_n) and denitrification of the nitrate in the water overlying the sediment (D_w) via incubation. The technique requires various assumptions:

a) The $^{14}NO_3^-$ and $^{15}NO_3^-$ in the sample pair randomly

b) Addition of ^{15}N tracer does not affect D_{14}

c) Labeled denitrification (D_{15}) is positively dependent on the $^{15}NO_3^-$ concentration

The same assumptions hold for natural DNRA ($DNRA_{14}$) and labeled DNRA ($DNRA_{15}$). These assumptions should be tested before data analysis. One method for this is to do parallel incubations with different concentrations of the tracer. (Nielsen 1992, Steingruber *et al.* 2001).

3. MATERIALS AND METHODS

3.1 Study site

The study lake, Lake Keurusselkä, is located in the city of Keuruu in Western Finland (Figure 2). It belongs to the Kokemäenjoki drainage system and has a watershed area of 1647 km² (Järviwiki 2014). The area of the lake excluding the islands is 97.56 km^2 and the mean depth is 4.66 m (OIVA ympäristö- ja paikkatietopalvelu 2014). Jaakonsuo municipal WWTP releases its effluent waters into the lake, and the effluent pipe is located in a 13 m deep bay where the water flows southwards. The treatment plant has been less efficient in N removal than in P removal (Table 2). The mean discharge in Lake Keurusselkä is 6.3 m^{-3} s^{-1}, so the dilution ratio of the wastewater is approximately 1:200 (Kokemäenjoen vesistön vesiensuojeluyhdistys 2011).

Table 2. Average nutrient loading from Jaakonsuo wastewater treatment plant during the years 1980-2010 (Kokemäenjoen vesistön vesiensuojeluyhdistys 2011).

	Wastewater (m^{-3} d^{-1})	Tot. P (µmol l^{-1})	Tot. P reduction (%)	Tot. N (µmol l^{-1})	Tot. N reduction (%)
Average	3406	16.33	92	1811.1	33
SD	699	4.42	2.8	458.3	12.7
Range	2710-4734	9.69-24.54	86-96	1071.4-2571.4	11-57

For the experiments, three sampling points were chosen according to their location in relation to the wastewater effluent pipe; point 1 was upstream of the pipe and was used as control, while point 2 was slightly to the south from the pipe head and point 3 further downstream (Figure 3). The sampling and experiments were carried out five times during the years 2013-2014 (Table 3).

Figure 2. Map of Finland (modified from Maanmittauslaitos 2014) and location of Keuruu shown by black dot.

Table 3. The sampling and experiment dates.

Samples collected	Incubation experiments
2 July 2013	3 July 2013
30 July 2013	31 July 2013
20 August 2013	21 August 2013
12 November 2013	13 November 2013
11 February 2014	12 February 2014

Figure 3. Map of the study lake and the three sampling points. The effluent pipe head is located just north of point 2 and the effluent is released southwards (modified from Maanmittauslaitos 2014).

3.2 Field data

The *in situ* vertical profiles (1 m depth intervals, starting from 1 m over the bottom) of dissolved O_2 concentration, temperature, conductivity, salinity and pH of the water column were measured using a YSI 6600 V2-4 CTD device from each sampling point. The exact depth of the points was also recorded. Water samples for NO_3^-, NO_2^-, NH_4^+ and phosphate (PO_4^{3-}) analyses were collected near the bottom with a 3 l Limnos water sampler. The samples were filtered (Whatman GF/C glass microfiber filters, pore size 1.2 µm) and frozen before analyses.

3.3 *In situ* experiments

Denitrification and DNRA were studied in the field using benthic flux chambers (approx. water and sediment capacities were 8.7 and 1.3 liters, respectively) that were specifically manufactured for this purpose (Figure 4). Three chambers were utilized in each measurement point. The chambers were reinforced with metal, so that they were heavy enough to slightly penetrate the sediment when released to the lake bottom. The chambers were connected to surface with ropes as well as a hose for sampling and injection purposes. Buoys were attached to the surface end. Once the chamber was set down, samples were collected from the hose with a syringe.

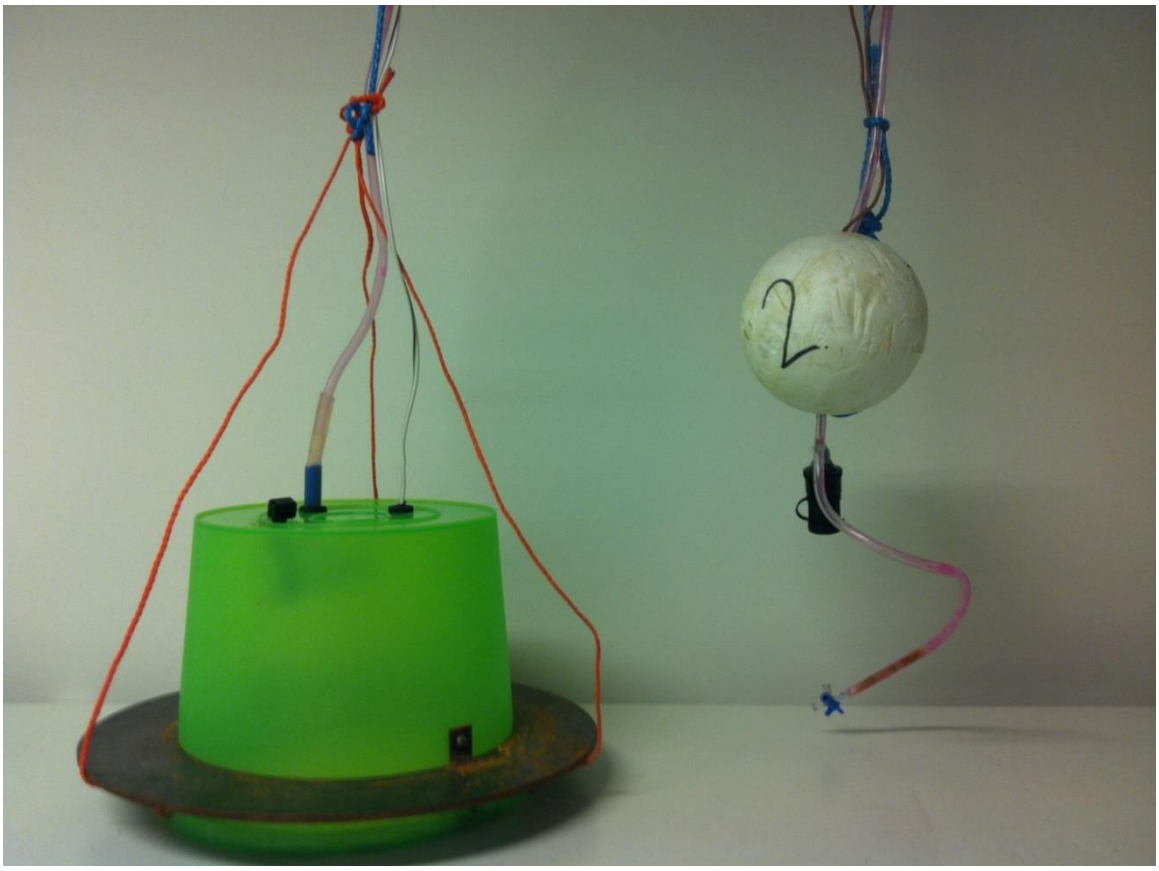

Figure 4. Benthic flux chamber and its buoy.

From each sampling point, six 12 ml samples were collected for N_2 and N_2O isotope ratio analyses, two 100 ml samples were collected for DNRA and nutrient content analyses and three 60 ml samples were collected for N_2O initial concentration analyses. $^{15}NO_3^-$ /rhodamine B –mixture was injected into the chamber via the hose. $^{15}NO_3^-$ solution was prepared from $K^{15}NO_3^-$ (^{15}N-% > 98 %, Cambridge Stable Isotope Laboratories). The water and rhodamine inside the chamber were mixed with an attached pump. The initial and final concentrations of rhodamine B were used to determine how much the chamber leaks. The target concentrations were 100 µmol l^{-1} for $^{15}NO_3^-$ and 1 mg l^{-1} for rhodamine B. After the injection and mixing, 1 dl sample was collected for determining the actual concentrations of the $^{15}NO_3^-$ and rhodamine B in the chamber.

After 4 hours of incubation, six 12 ml samples were collected for the N_2 and N_2O isotope ratio analyses, 100 ml sample was collected for the isotopic and concentration analysis of NH_4^+ (DNRA) and rhodamine B final concentration analyses and three 60 ml samples were collected for the N_2O final concentration analyses from each chamber. The samples were collected and stored in 12 ml exetainer vials (Labco Limited) (N_2 and N_2O), in 100 ml plastic containers (DNRA, nutrient content) and in 60 ml polypropylene syringes (N_2O initial and final concentrations). Further reactions in the exetainer vials were inhibited by adding 100 µl of 37% formaldehyde. All samples gathered in the whole experiment were immediately put on ice for transportation to laboratory. The DNRA and nutrient samples were filtered (Whatman GF/C glass microfiber filters, pore size 1.2 µm) and frozen in the laboratory. Before filtering, 1.5 ml subsamples were collected from DNRA samples of each point into Eppendorf tubes for rhodamine B final concentration analyses.

3.4 Sampling for incubation experiments

For *in vitro* experiments, sediment cores containing sediment and water overlying the sediment were sampled using plexiglass tubes (length 50 cm, ø 4.2 cm) attached to a KC Kajak Sediment Core sampler (Figure 5). Seven cores were collected from each point. The tubes were sealed with rubber stoppers at both ends and covered from sunlight with a black plastic bag. Once the field work was completed, the tubes were transported to laboratory where they were put into a refrigerator until the incubations. The temperature in the refrigerator was set to that of *in situ* above sediment surface.

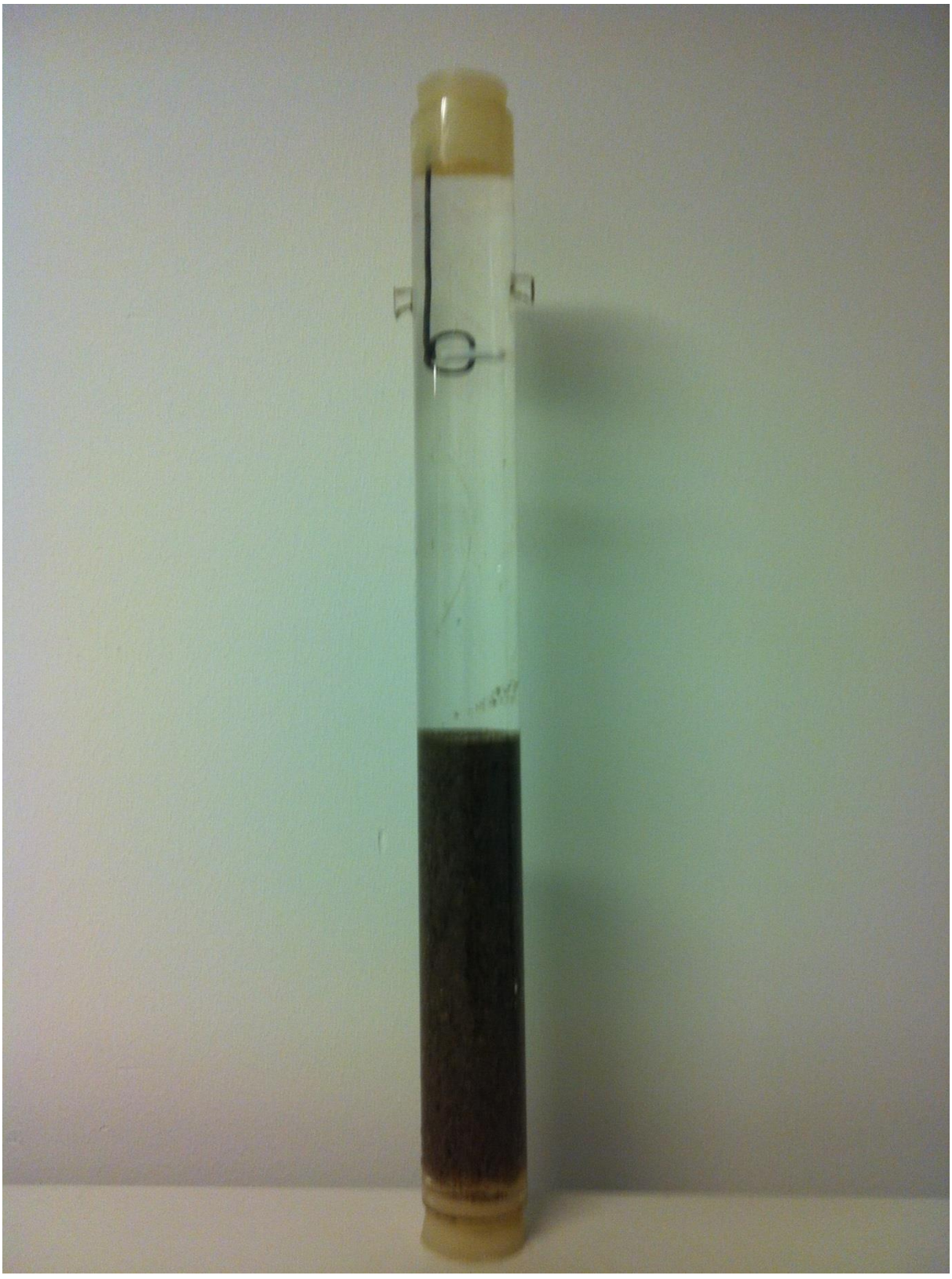

Figure 5. Plexiglass tube containing water/sediment sample and a magnetic stirrer used in the incubations.

3.5 Laboratory experiments

In the laboratory, five sediment cores of each sampling point were used for incubation experiments. Stock solution (0.1 mol l^{-1}) of K $^{15}NO_3^-$ (^{15}N-% > 98 %, Cambridge Stable Isotope Laboratories) was added to the incubation cores (Figure 5) according to the desired concentration and the volume of the water phase overlying the sediment inside the tube. In order to test the IPT assumptions, the incubations were conducted in five different concentrations of the stock solution in the cores: 25, 75, 150, 250 and 400 µmol l^{-1}. Thus each sampling point provided five tubes, which could be treated as replicates in the data analysis. The tubes were closed with rubber caps and incubated in dark and at constant *in situ* temperature for 4 hours. The water was constantly mixed with a magnetic stirrer attached to the rubber cap and driven by an external magnet.

After the incubation, the upper cap was removed, the water phase and sediment were mixed with a glass rod and the slurry was allowed to settle for a few minutes. From each incubation core, six 12 ml subsamples were collected into exetainers (Labco Limited) for the N_2 and N_2O isotope ratio analyses and further microbial activity was inhibited by adding 100 µl of 37% formaldehyde to the subsamples. For the isotopic and concentration analysis of NH_4^+ (DNRA), 60-100 ml subsamples were collected into 100 ml plastic containers. These subsamples were filtered (Whatman GF/C glass microfiber filters, pore size 1.2 µm) and frozen before analyses. For the N_2O concentration analyses, three 60 ml samples were collected into 60 ml syringes. The N_2, N_2O and DNRA samples were also collected from the background cores without any labeling. In addition, samples were collected from the two background cores for loss on ignition (LOI) and sediment porosity analyses.

3.6 Reactor experiments

The variations in denitrification and DNRA rates between different dilutions of wastewater were studied in a batch incubation experiment using ten continuous water flow reactors (height 67 cm, ø 9.5 cm) (Figure 6). The reactors were acclimatized in 5 different dilutions of wastewater for 16 days, after which denitrification and DNRA measurements were conducted in the same dilutions. The first experiment (25th February 2014) was a 24 hour time series experiment with sampling at eight hour intervals. The second experiment (27th February 2014) was a continuous 24 hour incubation, followed by a slurrying of the sediment in the reactors to determine how much gases are released in such a process. The concentration of NO_3^- was chosen to be the dilution variable. Actual wastewater (1857 µmol l^{-1} NO_3^- -N) from the Keuruu WWTP was used as a stock solution and groundwater was used to dilute it into 178.6, 357.1, 535.7, 714.3 and 892.9 µmol l^{-1} (2.5, 5, 7.5, 10 and 12.5 mg l^{-1}) NO_3^- -N. The five different dilutions and ten reactor units allowed for two replicates of each dilution.

$K^{15}NO_3^-$ powder was added to the reactors as a label for the determination of processes. Surface sediment was collected from Lake Keurusselkä (sampling point 2) using Ekman grab sampler and placed in the reactors to simulate *in situ* conditions. The heights of the water phases varied between 25 and 29.5 cm. Benthic invertebrates were removed from the sediment, after which it was homogenized by filtering it through a 0.5 mm mesh and placed inside the reactors. The volumes of sediment phases inside the reactors were from 0.78 to 0.92 dm^3 and the volumes of the water phases ranged from 1.77 to 2.09 dm^3. The diluted stock wastewater was pumped through the reactors with ten hoses running through a peristaltic pump (flow rates 148.0-157.6 ml h^{-1}).

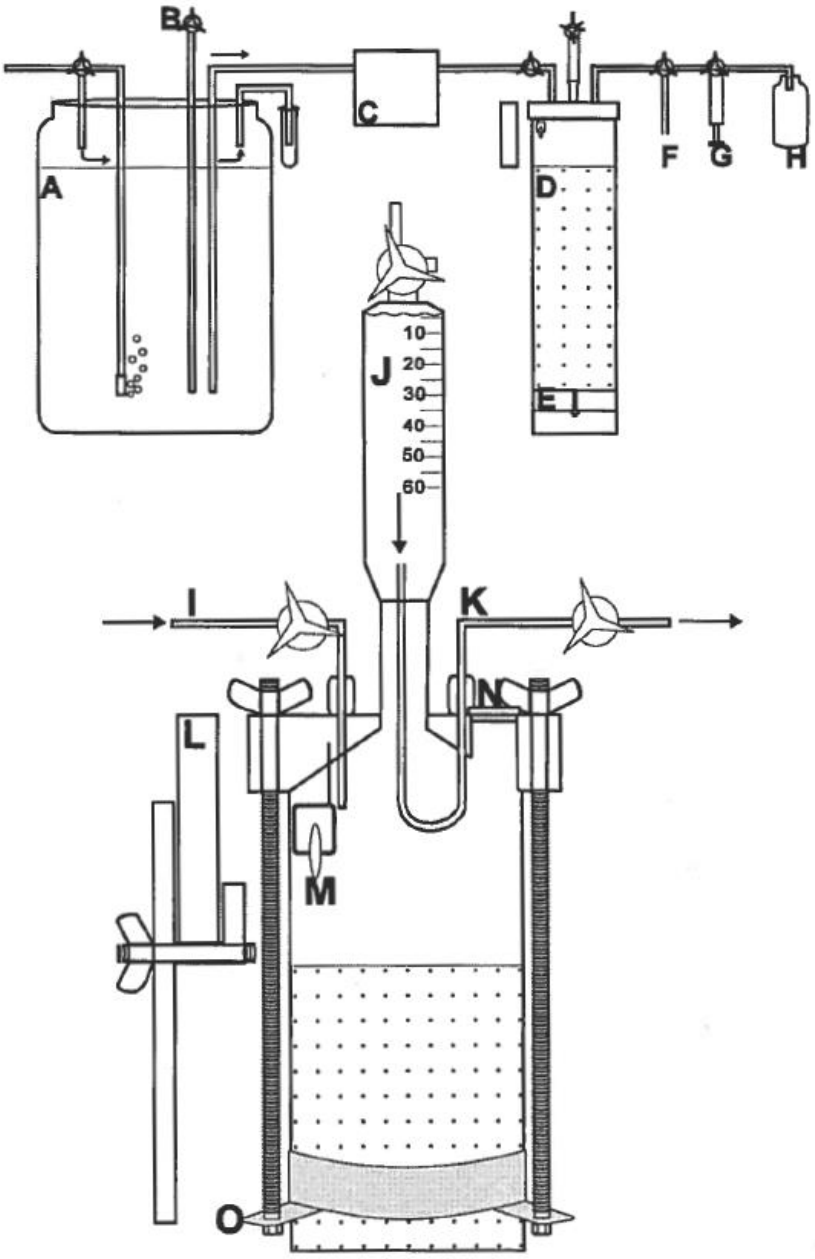

Figure 6. Schematic image of one reactor unit and its reservoir. A: reservoir, B: sampling outlet, C: peristaltic pump, D: sediment core, E: bottom cap, F: outflow to drain, G: sampling with syringe, H: sampling with bottle, I: inflow, J: gas trap, K: outflow, L: magnetic stirrer, M: rotating magnet, N: port for electrodes, O: removable clamp. Modified from Liikanen *et al.* 2002.

3.6.1 The procedures for the reactor experiments

During a 16-day preincubation period (27 January-11 February 2014), the quality of the outflowing water was allowed to stabilize so that the water quality parameters of the inflow, outflow and reactor waters did not fluctuate considerably (Table 4). Dissolved O_2 concentration, NO_3^-, conductivity and redox potential were measured daily inside the reactors, as well as from both inflow and outflow water using a Vernier LabQuest 2 interface and

applicable sensors. The used sediment was analysed for its water content, porosity and LOI. New dilutions of the stock wastewater were made whenever the water in the reservoir buckets started to run out. The NO_3^- concentration of the stock wastewater was measured with the Vernier LabQuest 2 and the dilutions were made accordingly.

Table 4. Qualities of the inflow, outflow and reactor waters before the experiments were started.

	O_2 mg l^{-1}	NO_3^--N mg l^{-1}	Conductivity µS cm^{-1}	Redox potential mV
Inflow				
2.5 mg l^{-1}	7.9	2.5	235	170
5 mg l^{-1}	7.8	5	321	185
7.5 mg l^{-1}	8.3	7.6	329	191
10 mg l^{-1}	8.1	10.1	412	195
12.5 mg l^{-1}	7.5	12.5	374	201
Outflow				
2.5 mg l^{-1}	7.7	3.1	224	200
5 mg l^{-1}	7.1	6	288	210
7.5 mg l^{-1}	6.2	10.2	367	217
10 mg l^{-1}	7.9	11.5	396	216
12.5 mg l^{-1}	7.3	12.1	393	217
Reactor (dilution)				
1 (2.5 mg l^{-1})	7.2	2.5	222	185
2 (5 mg l^{-1})	6.4	4.6	294	195
3 (7.5 mg l^{-1})	5.2	7.1	359	190
4 (10 mg l^{-1})	8.2	9.7	382	198
5 (12.5 mg l^{-1})	n/a	10.2	401	201
6 (2.5 mg l^{-1})	n/a	1.9	224	188
7 (5 mg l^{-1})	n/a	4.9	309	194
8 (7.5 mg l^{-1})	n/a	8.2	365	198
9 (10 mg l^{-1})	n/a	9.5	391	202
10 (12.5 mg l^{-1})	n/a	12.1	414	205

The background samplings were conducted after the stabilization period on 11th February 2014. Initially the reactors were disconnected from the peristaltic pump, and valves for both inflow and outflow were opened and 60 ml of sample water was squeezed into the system in order to expel all the water inside the tubings. The background samples for the isotopic analyses were collected into 12 ml exetainer vials (3 exetainers for N_2 and 3 exetainers for N_2O) and 100 µl of 37% formaldehyde was added to kill the microbial activity. The 30 ml background samples for determining the concentrations of N_2O were collected into 60 ml syringes. The 100 ml background samples for DNRA analyses were collected into 500 ml plastic bottles which were then frozen until analysis. In addition, 100 ml samples were collected for nutrient content analyses in 100 ml plastic containers. The DNRA and nutrient samples were filtered (Whatman GF/C glass microfiber filters, pore size 1.2 µm) and frozen before analyses. The inflow and outflow valves were closed after collecting the background samples.

The actual incubations were started by adding $K^{15}NO_3^-$ powder into the reactors with the desired fraction of $^{15}NO_3^-$ -N being approximately 10 % (Tables 5 and 6). However, the 10% concentration was not achieved in every reactor, which might be the result of malfunctioning NO_3^- probe or human errors in the wastewater dilutions.

Table 5. Required concentrations of $K^{15}NO_3^-$ powder in the five dilutions of stock wastewater.

Non-labelled NO_3^- -N (mg l^{-1})	$^{15}NO_3^-$ -N (mg l^{-1})	$K^{15}NO_3^-$ powder required (mg l^{-1})	Final NO_3^- -N (mg l^{-1})	Fraction of labelled NO_3^- -N
2.5	0.3	2.04	2.8	0.107
5	0.55	3.74	5.55	0.099
7.5	0.9	6.12	8.4	0.107
10	1.1	7.48	11.1	0.099
12.5	1.5	10.2	14	0.107

Table 6. Water phases and $K^{15}NO_3^-$ powder additions during the reactor experiments. Reactors 1-5 were used for dilutions of 2.5, 5, 7.5, 10 and 12.5 mg l^{-1} NO_3^- -N of the stock wastewater, and reactors 6-10 were the replicates in respective order. 1. exp. = time series incubation, 2. exp. = continuous incubation.

Reactor (dilution)	Water phase (dm^3)	Required amount of $K^{15}NO_3^-$ (mg)	$K^{15}NO_3^-$ added in 1. exp. (mg)	Fraction of labeled NO_3^- -N in 1. exp	$K^{15}NO_3^-$ added in 2. exp. (mg)	Fraction of labeled NO_3^- -N in 2. exp
1 (2.5 mg l^{-1})	1.95	3.97	3.80	0.120	3.92	0.124
2 (5 mg l^{-1})	1.88	7.02	7.10	0.097	7.13	0.113
3 (7.5 mg l^{-1})	1.88	11.49	11.37	0.075	11.40	0.097
4 (10 mg l^{-1})	1.91	14.31	14.28	0.061	14.32	0.128
5 (12.5 mg l^{-1})	1.98	20.23	20.19	0.064	20.38	0.091
6 (2.5 mg l^{-1})	1.95	3.97	3.90	0.114	3.85	0.032
7 (5 mg l^{-1})	1.98	7.42	7.45	0.094	7.55	0.041
8 (7.5 mg l^{-1})	1.77	10.84	10.77	0.069	10.91	0.076
9 (10 mg l^{-1})	2.09	15.63	15.59	0.064	15.60	0.057
10 (12.5 mg l^{-1})	2.06	20.96	20.88	0.066	20.92	0.067

The first sampling was conducted after 8 hours of incubation. The inflow and outflow valves were opened and 60 ml of sample water was squeezed to expel the water from the tubings. The N_2, N_2O and DNRA samples for the isotopic analyses were collected the same way as explained above for the background samples. The valves were again closed and the reactors were left to incubate. The second and third samplings were conducted after 16 and 24 hours of incubation and according to the same protocol. After the third sampling, the reactors were connected back to the peristaltic pump and the system was left running until the start of the second reactor experiment next day.

The continuous 24 hour incubation followed the same procedure, including collection of the background samples, but without the 8 and 16 hour interval samplings. After 24 hours of incubation the sediment in the reactors was slurried using a plastic stirring rod. The sediment was allowed to settle for a few minutes before conducting sampling for the N_2, N_2O and DNRA analyses as explained above.

3.7 Background data analyses

All of the nutrient analyses of this project were performed at Nab Labs Ltd. commercial laboratory in Jyväskylä. NO_3-N and NH_4-N analyses were made according to standards SFS-EN ISO 13395:1996 and SFS-EN ISO 11732:2005, respectively. The NO_2-N and PO_4-P analyses were done with in-house methods using automatic analyzers. The rhodamine B samples were pipetted into micro plates and the initial and final concentrations were analyzed with a PerkinElmer VICTOR X4 multilabel plate reader.

Sediment subsamples for the background analyses were gathered from the background cores with a hollow tube. Approximately 20 mm layers of sediment were collected into pre-

weighed 100 ml plastic containers and the wet weights were measured. Thereafter the containers were freeze-dried with a Christ Alpha 1-4 LD Plus device for 3 to 4 days. The dry weights of the samples were measured, after which they were heated in oven (450 °C, 4 h). The samples were weighed again for determining the LOI. The water contents and porosities of the subsamples were calculated using the following equations:

$$Water\ content = w\% = (wet\ weight - dry\ weight) \times \frac{100\%}{wet\ weight}$$

$$Porosity = p\% = \frac{(w\% \times \rho s)}{[100 + w\% \times (\rho s - 1)]}, \rho s = 2.6$$

3.8 Isotopic and concentration analyses of N_2 and N_2O and isotopic analysis of NH_4^+

3.8.1 N_2

Helium (He) was injected to the headspaces of the N_2 exetainers, as it was used as a carrier gas in the SIA. The exetainers were put underwater to avoid air contamination and 6 ml of water was replaced with He using a three-way stopcock and a 10 ml syringe. The exetainers were then put on a shaker table (150 rpm, 15 min), settled in a room temperature overnight and centrifuged (2000 g, 3 min). N_2 isotope ratios were determined with an Isoprime 100 IRMS device coupled with Trace Gas pre-concentrator. The device measured the concentration of N_2 in the samples, as well as the isotopic composition of N_2 ($^{28}N_2$, $^{29}N_2$ and $^{30}N_2$) using air as a standard.

3.8.2 N_2O

Isotopic analysis of N_2O was similar to the N_2 procedure, but after the first experiment it was noted that water samples in exetainers are not suitable for the N_2O isotope analysis due to low N_2O content in samples. Therefore, the 60 ml syringes which were originally meant for concentration analyses with gas chromatograph were used instead. 30 ml of helium was injected into the syringes and the exact volumes of both water and helium were recorded. The syringes were then put on a shaker table with 120 rpm for 5 minutes. Finally the gas phases were injected into vacuumed 12 ml exetainers. The N_2O isotope ratios were determined with an Isoprime 100 IRMS device coupled with Trace Gas pre-concentrator. The device measured the concentration of N_2O in the samples, as well as the isotopic composition of N_2O ($^{14}N^{15}N^{16}O$/$^{15}N^{14}N^{16}O$, $^{15}N^{15}N^{16}O$, $^{14}N^{14}N^{18}O$ and $^{14}N^{14}N^{16}O$) using N_2O gas a standard.

3.8.3 NH_4^+

The NH_4^+ analyses were done using a diffusion method, in which the NH_4^+ in an alkaline water sample is transformed to ammonia which is trapped into an enclosed filter paper saturated with acid. The method was adapted from Sigman *et al.* (1997). The "acid traps" consisted of three small pieces of filter paper cut with a hole punch and saturated with 20 µl of 2.5 M $KHSO_4$ inside two strips of Teflon tape. The traps were appended inside 250 ml glass bottles (approx. 2 cm from the mouth) containing 40 ml of the filtered water sample. 2 g of NaCl and 0.12 g of MgO were added to the samples to make them alkaline, and the pH was checked with Merck indicator paper. The bottles were closed with rubber septa caps and metallic tightening rings.

The bottles were put to a shaker (speed 120 rpm, temperature 35 °C) for 5 days. The filter pieces were then removed from the traps and put into 1.5 ml Eppendorf vials and into a desiccator, along with silica desiccant and a beaker containing 30 ml of 95% sulfuric acid, where they were left to dry for 24 hours. After this, the filters were prepared for the SIA, which was conducted with Thermo Finnigan Flash EA1112 elemental analyser connected to a Thermo Finnigan DELTA^{plus} Advantage stable isotope ratio mass spectrometer. The device measured the atomic percentage (AT%) of ^{15}N using ammonium sulfate and FSS2 (a fish standard manufactured from pike in the University of Jyväskylä) as standards.

3.9 Calculations

Volume of water in the IPT tubes (V_{wtot}) was calculated as:

$V_{wtot} = V_{wsed} + V_{wpore}$, where

$V_{wsed} =$ volume of water overlying the sediment $= A_s(h_{water} - h_{stopper})$;

$V_{wpore} =$ volume of porewater in the sediment $= A_s h_s \times p\%$;

$A_s =$ Area of the sediment $= \pi r^2$;

$h_s =$ height of the sediment phase $= h_{IPT} - (h_{water} + h_{stopper})$;

h_{water} = height of the water phase; $h_{stopper}$ = thickness of the stopper in the IPT tube; $p\%$ = sediment porosity; r = radius of the IPT tube; h_{ITP} = height of the IPT tube.

Rates of denitrification (Tuominen *et al.* 1998, Nielsen 1992) were calculated from the ratios of $^{29}N_2$ ($^{14}N^{15}N$) and $^{30}N_2$ ($^{15}N^{15}N$), which are formed during the IPT incubations. These were calculated by dividing the signals of $^{29}N_2$ and $^{30}N_2$, given by IRMS, by the signal of total N_2 ($^{28}N_2$+$^{29}N_2$+$^{30}N_2$). The isotopic ratios of non-incubated control samples (from background cores) were subtracted from those of incubated samples to calculate the excess ratios of $^{29}N_2$ and $^{30}N_2$ produced during incubations. These excess ratios were multiplied with total N_2 concentration (µmol l^{-1}) to calculate the excess concentration of $^{29}N_2$ (Dm_{29}) and $^{30}N_2$ (Dm_{30}). Thereafter, the concentration of excess ^{15}N-labelled gas was calculated as:

$d_{15} = Dm_{29} + 2 \times Dm_{30}$

and converted to production rate of ^{15}N-labelled N_2-gas as:

$D_{15}(\mu mol\ N\ m^{-2} d^{-1}) = \frac{d_{15} V_{wtot}}{0.0001 A_s \times \frac{T_{inc}}{60} \times 24}$, where

V_{wtot} = volume of water in the sample; A_s = area of the sediment in the sample (cm^2); T_{inc} = time of incubation (min).

Production rate of natural N_2 gas was then estimated based on IPT equations (Nielsen et al. 1992) as:

$$D_{14} = \frac{D_{15} \times Dm_{29}}{2 \times Dm_{30}}$$

IPT allows to distinguish between D_w (denitrification in the water overlying the sediment) and D_n (coupled nitrification-denitrification) as follows

$$D_w = \frac{D_{15}NO_{3_{orig}}}{NO_{3_{added}}}$$

$D_n = D_{14} - D_w$, where

NO_{3orig} = nitrate concentration in the water overlying the sediment; NO_{3added} = labeled nitrate concentration.

The AT% ^{15}N of NH_4^+ in the samples were divided by 100 and the concentration of the excess ^{15}N-NH_4^+ ($DNRA_{15}$) values were acquired by subtracting the background core values from those of the incubated sample and multiplying the result with the corresponging NH_4 -N concentration. The $DNRA_{15}$, $DNRA_{14}$, $DNRA_n$ and $DNRA_w$ values were calculated with the same principles as those of denitrification.

Only D_{15} and D_w were calculated for the reactor results, because no $^{30}N_2$ was formed during those experiments.

3.10 Statistical analyses

Correlations between the environmental factors (background data) and the rates of denitrification (D_{14}, D_n, D_w) and DNRA ($DNRA_{14}$, $DNRA_w$, $DNRA_n$) were studied with Spearman correlation analysis. In correlation analyses, site/season-specific average denitrification and DNRA values were used from all occassions when the IPT assumptions were met. To determine whether the rates were significantly different in the three sampling points and on five sampling occasions, either one-way analyses of variance (ANOVA) or t-tests were conducted, depending on the available data. The study methods provided five replicates from each point per sampling time, but in reality the number of replicates varied from 0 to 5. Testing was conducted whenever there were at least 3 replicates. The statistical analyses were done in SPSS Statistics 20.

4. RESULTS

4.1 Background data

The NH_4^+ and LOI values showed temporal and spatial fluctuation on all points throughout the study. Generally the NO_3^- and PO_4^- concentrations were highest in point 2 (effluent pipe), while point 1 (control) had the lowest values (Table 7). Exceptions occurred on 30 July ’13 when point 3 had lower NO_3^- concentrations than point 1, and PO_4^- concentration was highest in point 3 but lowest in point 2. Greatest overall NO_3^- and PO_4^- concentrations were observed in August and 30 July, respectively. The O_2 concentration and temperature were generally highest in the shallow control point during summertime, similar in all points on 12 November ’13 and lowest in point 3 on 11 February ’14. Overall O_2 concentrations were highest in November, when all points had values over 350 µmol l^{-1}. Temperature ranged between 15 and 20 °C during summertime, while November and February had much lower values. pH values ranged from 6 to 6.5 in all points during summer and winter, while on 12 November ’13 they were around 7 in all points.

4.2 Assumptions of IPT and DNRA measurement technique

The assumptions underlying isotope pairing technique were tested by plotting the denitrifications and DNRAs of both natural $^{14}NO_3^-$ (D_{14}; $DNRA_{14}$) and labeled $^{15}NO_3^-$ (D_{15}; $DNRA_{15}$) on graphs with the concentration of added $^{15}NO_3^-$ on the x-axis (Figures 7 and 8, appendix 1). For the assumptions to hold, D_{15} and $DNRA_{15}$ should show positive tendency, while D_{14} and $DNRA_{14}$ should not show positive tendency on added concentration of $^{15}NO_3^-$. The assumptions were not met on following occasions: 2 July '13 in sampling point 3 (no positive tendency on D_{15}), 30 July '13 in sampling point 2 (no positive tendency on D_{15}) and 11 February '14 in sampling point 2 (no positive tendency on D_{15} or $DNRA_{15}$; positive tendency on D_{14} and $DNRA_{14}$).

Table 7. Concentrations of NO_3^-, NH_4^+, PO_4^- and O_2, as well as temperature (*T*) , pH and LOI in the three sampling points during the five sampling times. LOI measured from sediment; other variables measured from water overlying the sediment. Point 1 = control, point 2 = effluent pipe, point 3 = downstream of the effluent pipe.

Point (depth)	NO_3^- (µmol l^{-1})	NH_4^+ (µmol l^{-1})	PO_4^- (µmol l^{-1})	O_2 (µmol l^{-1})	*T* (°C)	pH	LOI (%)
2 July '13							
1 (4 m)	9.28	6.64	0.81	250.13	19	6.49	18.98
2 (10 m)	92.8	32.86	1.87	257.94	15.8	6.07	17.01
3 (7 m)	32.13	32.14	1.19	218.59	16.8	6.36	16.06
30 July '13							
1 (4 m)	22.13	20.71	3.23	250.13	19	6.48	14.91
2 (10 m)	56.4	34.29	2.55	192.36	15.82	6.19	18.23
3 (7 m)	15.71	40.71	4.52	218.59	16.58	6.36	17.04
20 August '13							
1 (4 m)	37.84	9.29	0.68	248.25	18.74	6.46	17.52
2 (10 m)	171.35	65.71	4.84	191.42	15.8	6.17	18.61
3 (7 m)	114.24	17.14	1.03	217.65	16.52	6.38	14.92
12 November '13							
1 (4 m)	11.42	15.71	0.81	352.55	4.05	7.04	19.64
2 (10 m)	135.66	5.21	1.52	350.68	4.18	7.09	14.81
3 (7 m)	46.41	6.21	1.23	350.68	4.18	6.96	18.79
11 February '14							
1 (4 m)	14.99	9.29	0.74	333.19	2.93	6.7	19.61
2 (10 m)	185.63	17.14	1.42	307.27	3.29	6.59	22.14
3 (7 m)	21.42	14.29	0.84	275.73	1.89	6.4	15.48

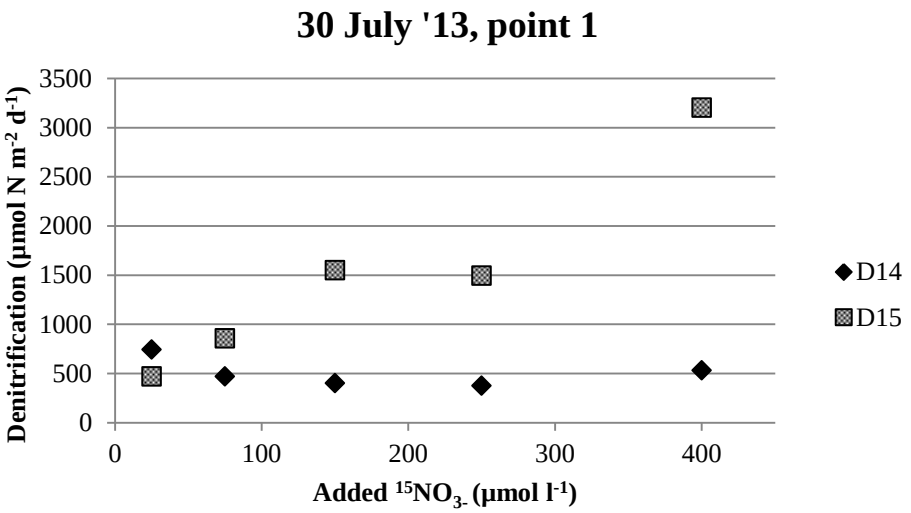

Figure 7. An example of a successful test of IPT assumptions showing the positive dependency between D_{15} and the added $^{15}NO_3^-$, while D14 remains relatively constant.

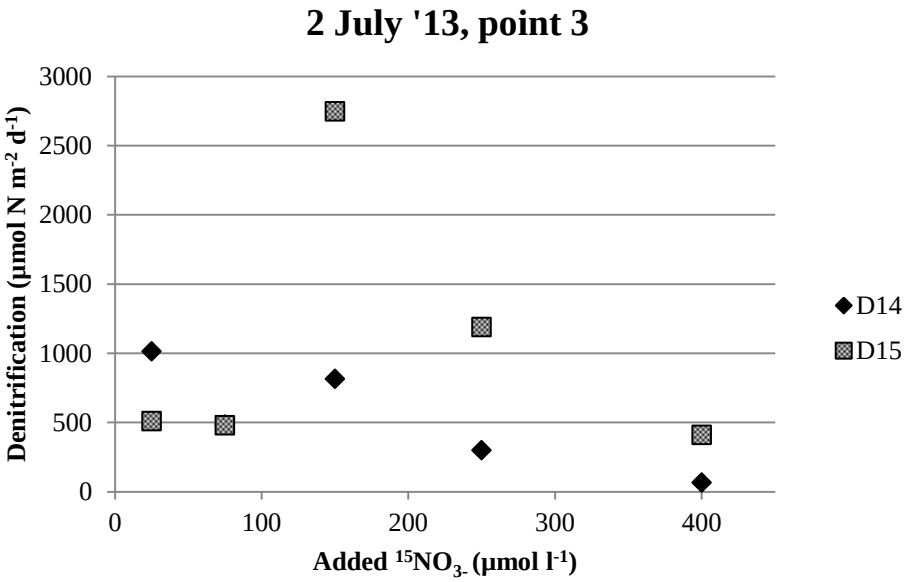

Figure 8. An example of an unsuccessful test of IPT assumptions showing no positive dependency between D_{15} and the added $^{15}NO_3^-$.

4.3 Rates of denitrification and DNRA

The average Dn and Dw rates in the sampling points varied from 106.9 to 4931.4 µmol N m^{-2} d^{-1} and from 49.0 to 4743.6 µmol N m^{-2} d^{-1}, respectively (Figure 9). The average DNRAn and DNRAw rates in the sampling points varied from 11.6 to 5274.0 µmol N m^{-2} d^{-1} and from 4.3 to 940.3 µmol N m^{-2} d^{-1}, respectively (Figure 10). The average rates of natural denitrification (D_{14}) and DNRA ($DNRA_{14}$) in the sampling points ranged from 159.3 to 5889.4

µmol N m^{-2} d^{-1} and from 15.5 to 6109.0 µmol N m^{-2} d^{-1}, respectively (Table 8 & Figure 11). The mean rates of denitrification in points 1, 2 and 3 during the whole study were 505.9 (n=5, SD=515), 3863.3 (n=4, SD=2288.7) and 546.5 (n=4, SD=129.9) µmol N m^{-2} d^{-1}, respectively. The corresponding mean DNRA rates were 147.8 (n=5, SD=148.2), 1833.5 (n=4, SD=2852.7) and 197.4 (n=4, SD=237.8) µmol N m^{-2} d^{-1}.

The Dn:Dw and DNRAn:DNRAw ratios varied in all points throughout the study; The Dn and DNRAn processes were mostly dominating. D_w and $DNRA_w$ were more active in point 2 (except on 12 February). Denitrification also dominated over DNRA (except in February '14, when DNRA activity in point 2 exceeded that of denitrification). The DNRA:denitrification ratio varied from 0.12 to 1.53 (mean 0.43) with no significant differences between sampling points or times. The portion of DNRA from the total NO_3^- removal (DNRA+denitrification) varied from 9 % to 52 % (mean 22 %) (Figure 11). The DNRA rates ranged from 15.48 to 383.39 µmol N m^{-2} d^{-1} in point 1, from 289.49 to 6108.96 N m^{-2} d^{-1} in point 2 and from 63.23 to 553.75 µmol N m^{-2} d^{-1} in point 3. In July and August, the DNRA rates ranged from 63.23 to 568.65 (n=8, SD=174.67) µmol N m^{-2} d^{-1} and during wintertime the rates varied between 15.48 and 6108.96 (n=5, SD=2664.91) µmol N m^{-2} d^{-1}.

Rates of denitrification at the effluent pipe were higher than those in the control point ($F=7.687$, $p<0.05$ on 2 July; $F=9.484$, $p<0.01$ on 30 July; $t=-4.352$, $p<0.01$ on 20 August; $F=11.500$, $p<0.01$ on 12 February). The denitrification rates were also significantly higher at the effluent pipe than in point 3 on 30 July ($p<0.05$) and 12 February ($p<0.01$). On 12 February, the DNRA activity in point 2 was significantly higher than in points 1 ($F=10.353$, $p<0.01$) and 3 ($p<0.05$), and on July 30 it was significantly higher at the effluent pipe than in point 3 ($F=5.472$, $p<0.05$).

The denitrification rates were always higher than the DNRA rates, except in February '14, when DNRA activity in point 2 exceeded that of denitrification. In point 1, DNRA performed better during July and August than in November and February ($t=3.113$, $p<0.01$). Rates of denitrification showed positive correlation with NO_3^- concentration ($r_s=0.782$, $p<0.01$) (Figures 12 and 13) and negative correlation with O_2 concentration ($r_s=-0.711$, $p<0.05$) and pH ($r_s=-0.891$, $p<0.01$) (Figure 14). Rates of DNRA correlated negatively with pH ($r_s=-0.644$, $p<0.05$) (Figure 15). Other correlations between the processes and environmental factors were not significant. The results exclude problematic data which was caused by malfunction of the IRMS device, missing samples and failures in the ^{15}N tracer method. More detailed discussion about the problematic data can be found in chapter 5. The results of the benthic flux chamber experiments and N_2O analyses will be presented in the Master's thesis of Felipe Muñoz Arraño.

Table 8. Average NO_3^- concentrations and rates of denitrification and DNRA during the whole study. *n/a*: data not available.

Point (depth)	NO_3^- (µmol l^{-1})	Denitrification (µmol N m^{-2} d^{-1})	DNRA (µmol N m^{-2} d^{-1})
2 July '13			
1 (4 m)	9.28	275.04	162.24
2 (10 m)	92.8	2997.90	366.98
3 (7 m)	32.13	534.79	63.23
30 July '13			
1 (4 m)	22.13	504.49	151.41
2 (10 m)	56.4	1026.04	289.49
3 (7 m)	15.71	668.74	84.78
20 August '13			
1 (4 m)	37.84	1395.23	383.39
2 (10 m)	171.35	5889.40	568.65
3 (7 m)	114.24	n/a	n/a
12 November '13			
1 (4 m)	11.42	195.20	26.68
2 (10 m)	135.66	n/a	n/a
3 (7 m)	46.41	370.03	87.68
11 February '14			
1 (4 m)	14.99	159.34	15.48
2 (10 m)	185.63	5539.81	6108.96
3 (7 m)	21.42	612.59	553.75

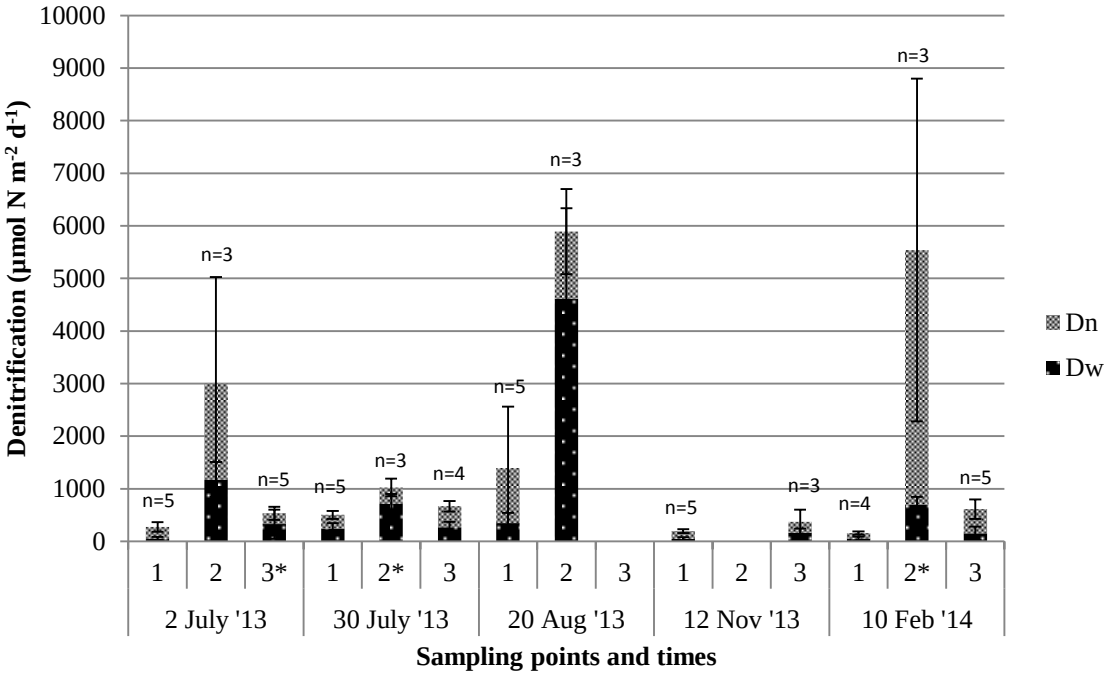

Figure 9. Rates of denitrification (average +/- SD) in the three sampling points during the five sampling occasions. *Dn*: coupled nitrification-denitrification; *Dw*: denitrification of the NO_3^- in the water overlying the sediment. Data not available for point 3 in 20 Aug '13 and point 2 in 12 Nov '13. The occasions when the IPT assumptions were not met are marked with an asterisk.

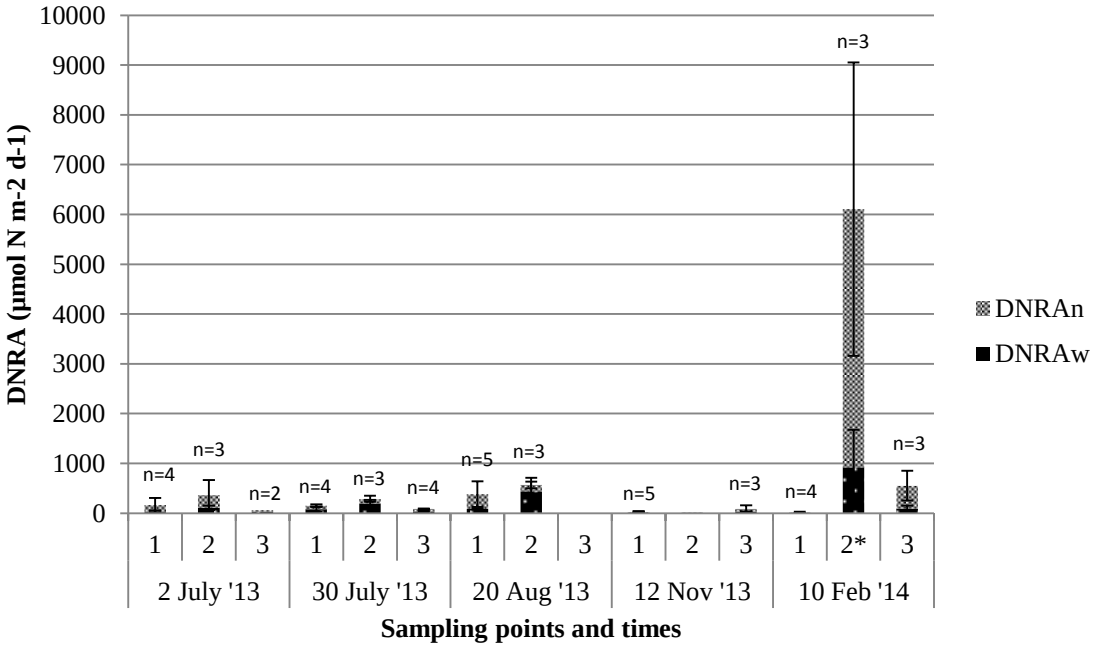

Figure 10. Rates of DNRA (average +/- SD) in the three sampling points during the five sampling occasions. *DNRAn*: DNRA of nitrate produced via nitrification; *DNRAw*: DNRA of nitrate in the water

overlying the sediment. Data not available for point 3 in 20 Aug ’13 and point 2 in 12 Nov ‘13. The occasions when the IPT assumptions were not met are marked with an asterisk.

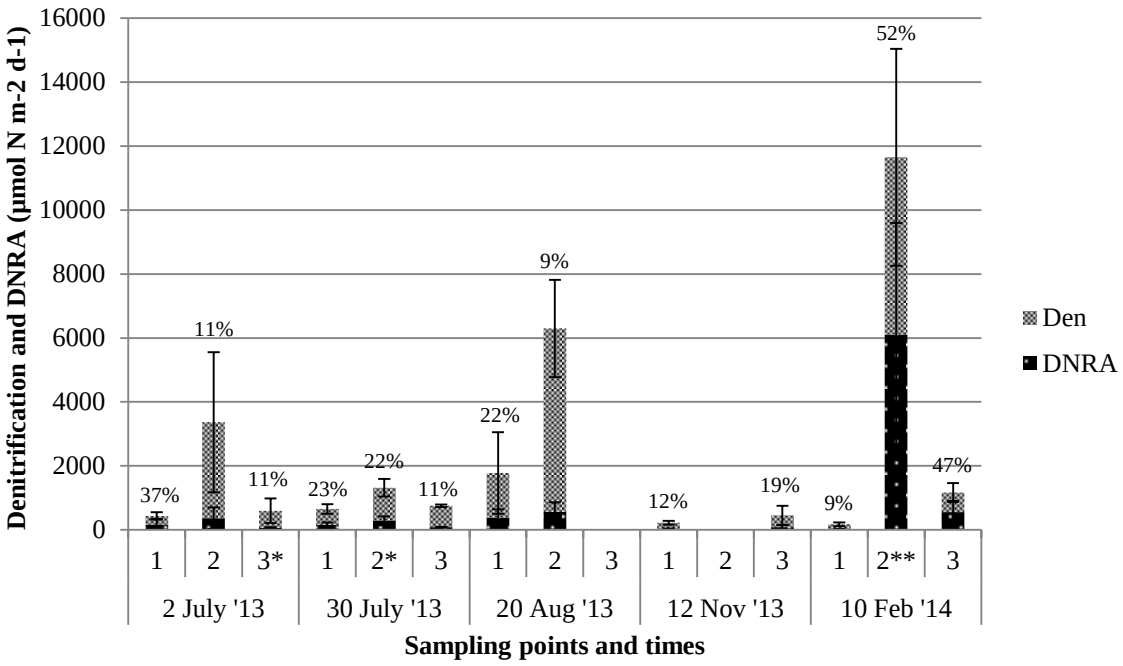

Figure 11. Rates of denitrification and DNRA (average +/- SD) in the three sampling points during the five sampling occasions. The fractions of DNRA from the total NO_3^- removal are marked on top of the columns. Data not available for point 3 in 20 Aug ’13 and point 2 in 12 Nov ‘13. The occasions when the IPT assumptions were not met are marked with an asterisk.

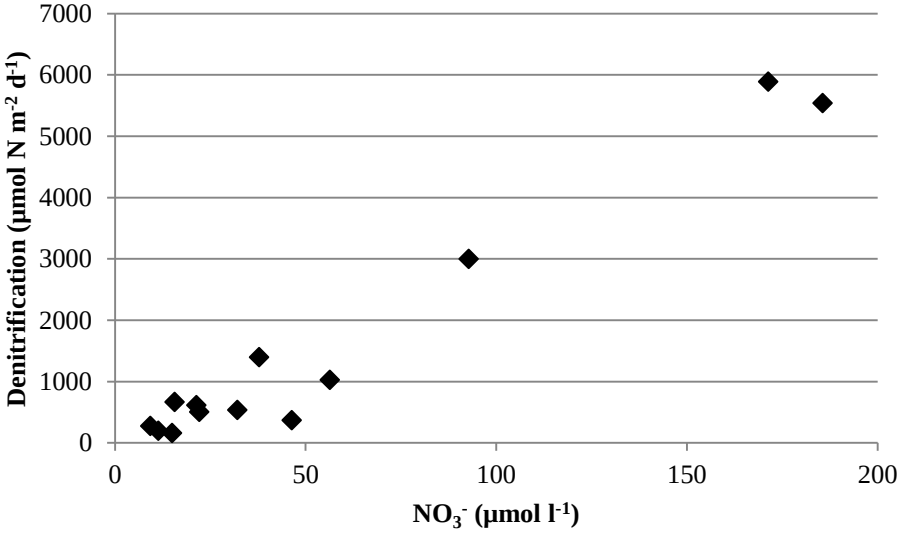

Figure 12. Correlation of the mean rates of denitrification with NO_3^- concentrations in all sampling points.

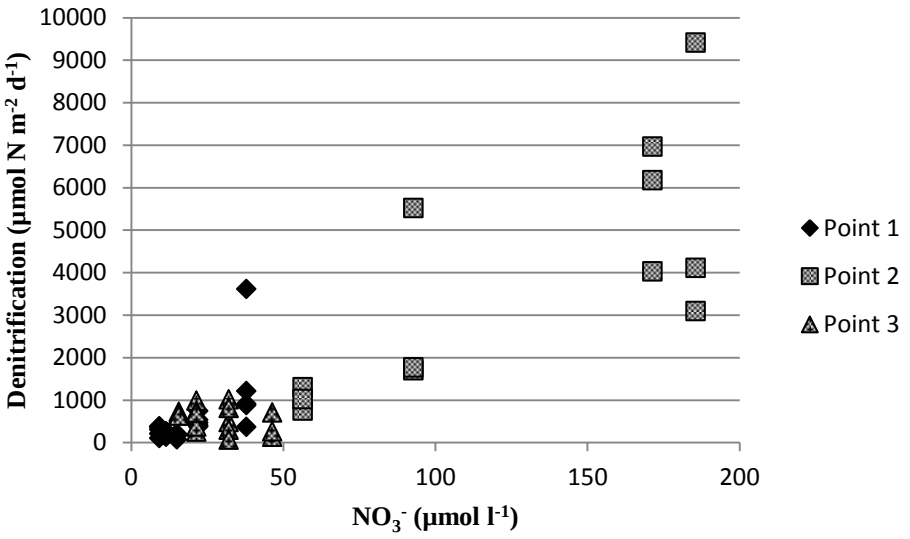

Figure 13. Correlation of the rates of denitrification with NO_3^- concentrations in the different sampling points, including all available replicate values.

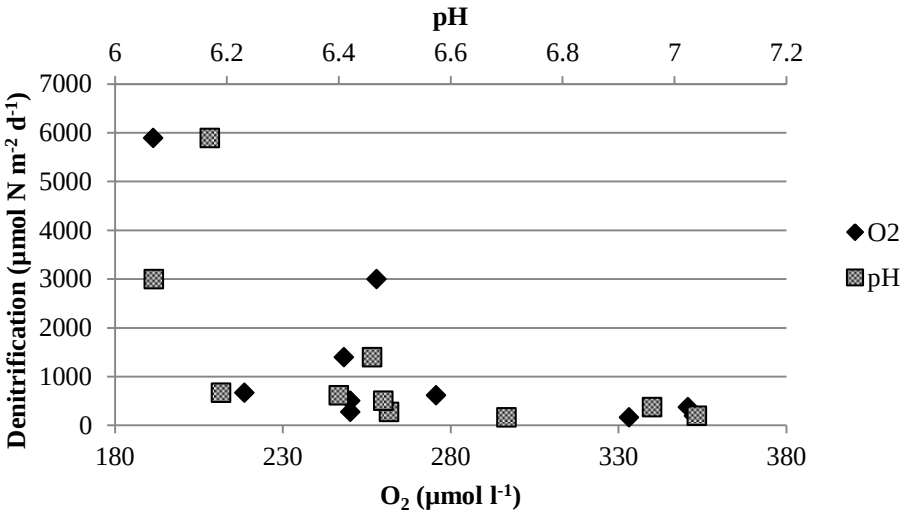

Figure 14. Correlations of the rates of denitrification with O_2 concentrations and pH.

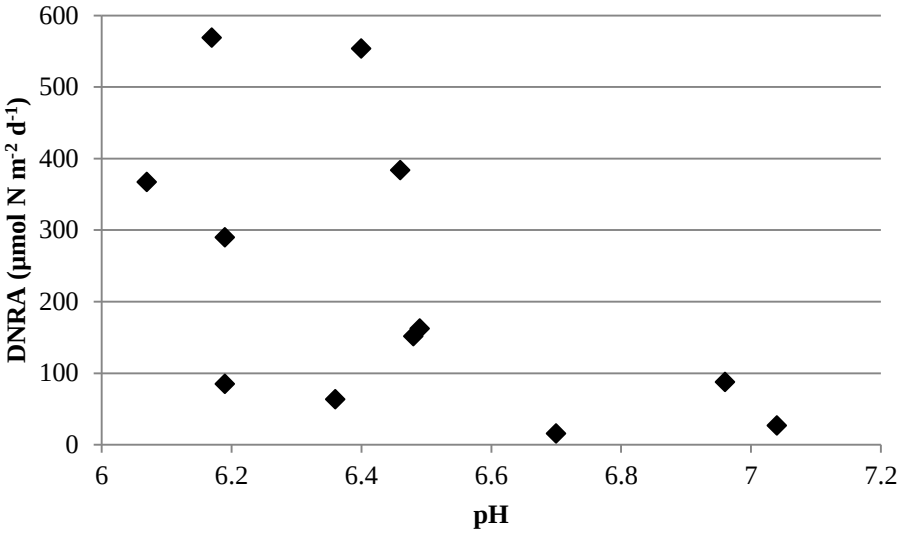

Figure 15. Correlation of the rates of DNRA with pH.

4.4 Reactor experiments

The D_{15} correlated only slightly with tracer additions after the first 8 h interval in the time-series experiment (Figure 16). There was no positive correlation after 16 or 24 hours of incubation. The D_w showed positive correlation with ambient NO_3^- levels after 8 and 16 hours, but not anymore after 24 hours (Figure 17). Positive correlations between D_{15} and amounts of tracer, as well as between D_w and ambient NO_3^- were observed in the 24 h experiment (Figures 18 & 19). The correlation was stronger in the latter one. The 24 h results were quite scattered in both experiments. The mean rates of D_{15} and D_w ranged respectively from 8.37 to 113.48 (n=29, SD=29.75) µmol N m^{-2} d^{-1} and from 87.7 to 1140.26 (n=29, SD=311.44) µmol N m^{-2} d^{-1} in the time-series experiment. The corresponding mean-rate variations in the 24 h experiment were from 41.98 to 153.09 (n=10, SD=34.35) µmol N m^{-2} d^{-1} and from 351.46 to 1858.62 (n=10, SD=586.85) µmol N m^{-2} d^{-1}.

The IRMS data from the reactor experiments did not yield usable DNRA results due to too small amount of $^{15}NO_3^-$ used. No DNRA activity could be observed in the SIA, because the IRMS device was unable to detect such low production rates.

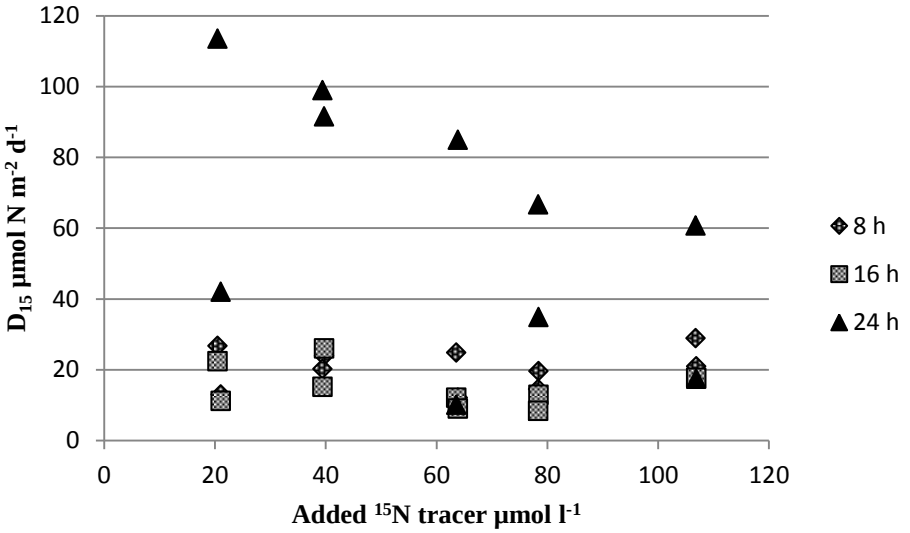

Figure 16. Tracer additions and labeled denitrification in the time-series reactor experiment.

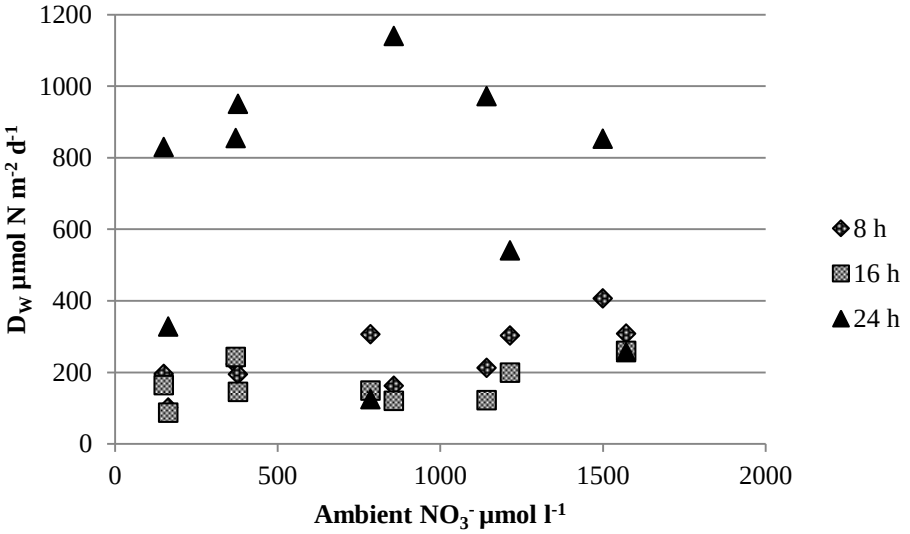

Figure 17. Ambient NO_3^- levels and denitrification of the water overlying the sediment in the time-series reactor experiment.

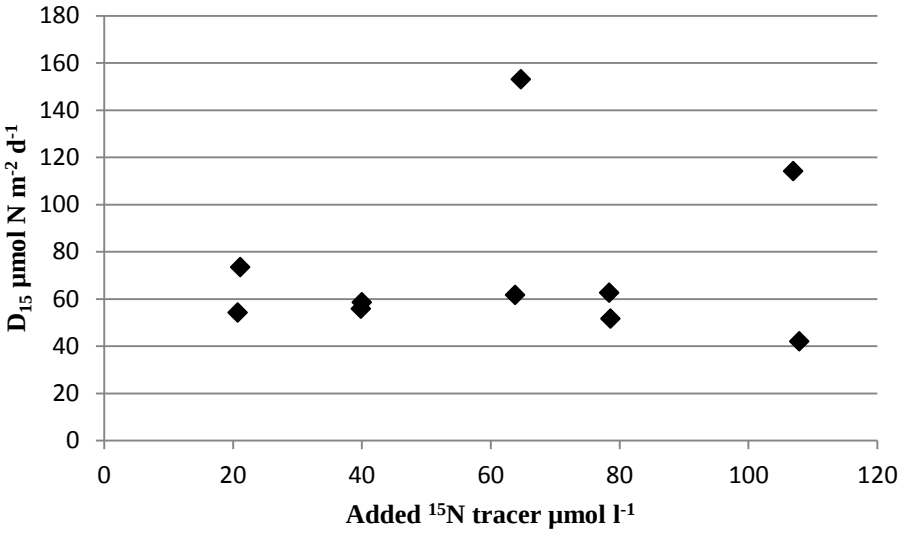

Figure 18. Tracer additions and labeled denitrification in the 24 h reactor experiment.

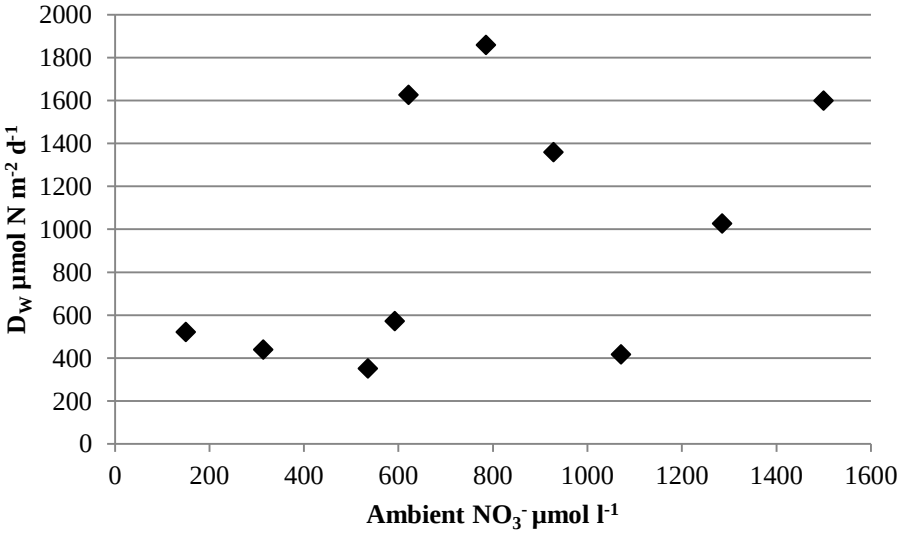

Figure 19. Ambient NO_3^- levels and denitrification of the water overlying the sediment in the 24 h reactor experiment.

5. DISCUSSION

Part of the data had to be excluded from the results due to the IPT method not working properly. Problems occurred especially in samples with higher NO_3^- concentrations (points 2 and 3), resulting in D_w values >100% of total denitrification in calculations and/or failures in the IPT assumptions. This would suggest that the IPT method, as such, is not suitable for determining the rates of denitrification or DNRA in samples with such high NO_3^- content. IPT has previously been applied to samples with considerably lower NO_3^- concentrations, and thus

these problems were not anticipated. Greater tracer additions could yield more viable results, as previous studies have shown that insufficient tracer additions can lead to errors in denitrification measurements (Minjeaud *et al.* 2008).

The reason for the extreme D_w values might be that the $^{14}NO_3^-$ and $^{15}NO_3^-$ in the IPT tubes were not homogenously mixed, and/or the water in the sample was not mixed properly during the incubations. There were occasional difficulties in getting the magnetic stirrers to function, and in samples with lower sediment phases the effect of the stirrers might not reach the lower parts of the sample. However, the *in situ* process rates could be so heterogenous that a concentration series of five tubes might not yield successful tests of the assumptions. Data from occasions when the assumptions were not met was thus included in the results. Since some of the concentration series provided better correlations than others, it is likely that the inadequate mixing is the culprit. In the future, special attention should be paid to how the water in the samples could be mixed properly; is it possible to attach a more efficient stirrer to the bottom of the top stopper in the IPT tube? The two lower tracer additions (25 and 75 µmol l^{-1}) were more problematic than the others, and thus the ^{15}N concentration series could be increased (for example 150, 250, 400, 600 and 850 µmol l^{-1}). On the other hand, too high concentrations increase the possibility that the system becomes saturated. If successful tests of assumptions can be conducted, the saturation point could be estimated. It would then be possible to determine a single tracer concentration that is safe to use in these conditions, which would obviate the need for the parallel dilutions.

The target fraction for the tracer in the reactor experiments (10%) was not achieved in each reactor, which was likely due to malfunctioning probes or human errors during the wastewater dilutions. The Vernier LabQuest 2 might not be the best available device for measuring wastewater because of the high NO_3^- concentration, which most likely caused the malfunctioning. Diluting the wastewater further for the measurements could have helped, but this would have caused extra work to an already intensive procedure and the experiment would have become unfeasible. A good option would be to measure the NO_3^- concentration of the raw wastewater, prepare the dilutions beforehand and freeze them until use, as opposed to making daily measurements and dilutions on the go. A probe designed specifically for wastewater measurements could also be used in the measurements. The IRMS device was unable to detect any $^{30}N_2$ production or DNRA activity, which could be because of inadequate tracer additions. Again, the amount of tracer could be increased, for example to 30% of the total NO_3^--N.

There were three people doing the field and laboratory work together, with varying individual tasks on different occasions. This definitely leads to some differences between the experiment procedures. Moreover, most of the tasks were completely new to the two Master's students involved. This together with the long working days increased the possibility of human error during the study. It was not possible to use the exact same devices, laboratories and other resources each time, which might have had minor impacts on the measurements as well.

High denitrification activity in point 2 together with the correlation analysis indicates that denitrification was mainly limited by the availability of NO_3^-. Correlations also showed that denitrification performed better in more anoxic conditions, as well as during lower pH, which is in agreement with previous findings (Rissanen *et al.* 2011, Song *et al.* 2013). DNRA did not show such overall trends; lower pH resulted in higher activity but there were only few

observations of significantly greater rates at the effluent pipe. DNRA rates in the control point were higher during the summer months, which could indicate that warmer temperatures are important for this process. Similar observation was made by Scott *et al.* (2008), who suggested that DNRA contributes to NO_3^- transformation in a freshwater wetland especially during summer months, with potential rates ranging from 24 to 792 µmol N m^{-2} d^{-1}. In Lake Keurusselkä, the higher D_w and $DNRA_w$ rates in point 2 as well as denitrification dominating over DNRA suggest that the NO_3^- in the wastewater effluent is utilized by both processes, but mostly by denitrification. The high rates in February '14 (points 2 & 3) are striking. The amount of NO_3^- at the time was not considerably bigger than in August or November and there was no sign of lower temperature inhibiting denitrification, as was suggested by Holmroos *et al.* (2012) in Lake Kirkkojärvi. The source of NO_3^- on this occasion was mostly nitrification instead of the wastewater effluent (Figures 9 & 10). This could be due to higher concentration of O_2 penetrating into the otherwise anoxic parts of the sediment, which can increase the rate of D_n and decrease the rate of D_w (Cornwell *et al.* 1999). The O_2 concentrations were indeed high on February (Table 7), even though this was the only occasion during the study when there was ice covering Lake Keurusselkä. The LOI on point 2 was also high in February, but statistical analyses showed no correlation between the organic matter content and the N transforming processes, contrary to what has previously been reported (e.g. Tomaszek & Gruca-Rokosz 2007, Han *et al.* 2014, Song *et al.* 2014). However, increasing the C/N ratio has not always yielded greater DNRA rates, which indicates that microbes do not necessarily utilize the most energy-efficient processes (Behrendt *et al.* 2014). Higher temperatures have generally enhanced denitrification (e.g. Warneke *et al.* 2011, Misiti *et al.* 2011), but in this study no significant link between temperature and the process rates was observed. Both denitrification and DNRA rates were high even in the cold conditions of February.

The mean denitrification rates in the control point and point 3 were higher than those previously observed in boreal lakes (Table 1). The high rates in point 1 can not be attributed to higher NO_3^- concentrations, but that is likely the reason for the results in point 3. The rates in point 2 were significantly higher due to the presence of the effluent pipe. DNRA rates were also higher than those observed in other studies; a Danish fjord with heavy aquaculture had DNRA rates ranging from 0 to 70 µmol N m^{-2} d^{-1} and DNRA/denitrification ratio of 0.25 (Christensen *et al.* 2000), while the findings of Nizzoli *et al.* (2010) showed DNRA rates of 24-216 µmol N m^{-2} d^{-1} in two mediterranean lakes, with DNRA/denitrification ratios ranging from 0.03 to 0.2. In relation to denitrification, DNRA was less active in these cases than in Lake Keurusselkä. The fraction of DNRA from the total NO_3^- reduction in this study was generally higher than in previous studies (e.g. Marchant *et al.* 2014). Higher DNRA rates in freshwater have been linked with high sulfide concentrations (Brunet & Garcia-Gil 1996), and some sulfate-reducing bacteria are indeed capable of DNRA (Rysgaard *et al.* 1996). The possible presence of these bacteria in Lake Keurusselkä should be assessed in further studies. Lake Keurusselkä might also have conditions that provide longer microbial generation times, which can result in better DNRA performance (Kraft *et al.* 2014).

D_{15} in the time-series reactor experiment increased along with tracer additions only in the beginning, and the correlation became negative over time. The sediments in the reactors might have become saturated as a result of the high levels of NO_3^-, and therefore the rates of denitrification did not increase in the end. Similar trend could be seen in some IPT incubations (Appendix 1), but to a lesser extent; the wastewater becomes more diluted in nature than in the reactors and thus the NO_3^- concentrations in the reactors are higher. Since the D_w calculations

are based on the assumption that D_{15} increases with the tracer additions, the D_w results have to be interpreted with caution. Both D_{15} and D_w rates were greater and more scattered at the 24 h point than after 8 or 16 hours. It seems that the denitrification rates accelerated during the experiment, but this could also mean that more trapped N_2 was released from the sediment over the course of the incubation. The IPT results show similar scattering in the natural denitrification rates of point 2 (Figure 13), where the NO_3^- concentrations were highest.

Stronger correlations were observed in the 24 h experiment, which was conducted just after the time-series experiment and using the same sediments in the reactors. The difference is likely caused by the slurrying of the sediments, which also resulted in greater rates of denitrification compared to the ones observed during the time-series experiment. Despite the higher NO_3^- concentrations, D_w rates in the reactor experiments were not as high as the peak values of point 2 in the IPT incubations (Figure 9). This suggests that the NO_3^- in the reactors was not transformed as much as *in situ*, or that is was mostly used by DNRA. In future studies, greater tracer additions should be applied so that the magnitudes of the different NO_3^- transformations could be determined. The wastewater could also be more diluted to prevent the possible saturation and to yield more accurate results when using the measuring probes. Without the saturation, the D_{15} would likely respond better to tracer additions, and the results would be overall more reliable. The effect of different retention times in the reactors should also be studied; longer retention can improve NO_3^- removal (Zhang *et al.* 2013, Harrison *et al.* 2014).

Based on the results of this thesis, the N transforming processes in Lake Keurusselkä seemed to be overall more active than in other previously studied boreal lakes. The hypothesis a) can be accepted since denitrification was highest in point 2, where the NO_3^- concentrations were higher due to the wastewater effluent. This is backed up by the reactor experiment results; D_w rates correlated with ambient NO_3^- levels, but longer incubation periods lead to saturation of the system. Hypothesis b) can not be accepted, since there were no significant differences in the DNRA:Den ratio within observations. The NO_3^- from the wastewater effluent accelerated the denitrification rate, but had no considerable effect on DNRA. DNRA still remains a less known process, but it seems that it does not considerably affect the natural purification of wastewater effluent via denitrification in Lake Keurusselkä.

ACKNOWLEDGEMENTS

When I started working on this thesis I had zero knowledge of the microbial processes in question, so I have had a lot to learn. My supervisors Professor Marja Tiirola and Dr. Antti Rissanen have been essential in helping me to understand the topic both as a whole and in detail. Marja assigned me to do the thesis and gave valuable background information by guiding me through the literature review and book examination. Upon the actual writing process, Antti provided me with endless feedback and comments. In addition to shaping the actual thesis, these conversations ensured that I learned new things throughout the whole project.

The other members of our research team, Ville Juusela and Felipe Muñoz Arraño, were equally important. The field and laboratory work was quite intense and extensive, with up to 18 hour days, so it was crucial that there was a functioning group who got along well. Ville was overseeing us on the field and in the lab, and thus he could give me valuable reminders as

to what was actually done and why. Thank you also to Dr. Sanni Aalto for consulting me with the IRMS data, to Dr. Hannu Nykänen for acting as the second reviewer and to *Maa –ja vesitekniikan tuki ry.* for the financial support.

I want to thank my family, friends and especially Anni for the constant support during this project. I would not have gotten this far without you.

REFERENCES

Abe K., Komada M., Ookuma A., Itahashi S. & Banzai K. 2014. Purification performance of a shallow free-water-surface constructed wetland receiving secondary effluent for about 5 years. *Ecol. Eng.* 69: 126-133.

Ahlgren I., Sörensson F., Waara T. & Vrede K. 1994. Nitrogen budgets in relation to microbial transformations in lakes. *Ambio.* 23: 367-377.

Andersson J.L., Bastviken S.K. & Tonderski K.S. 2005. Free water surface wetlands for wastewater treatment in Sweden – nitrogen and phosphorus removal. *Water Sci. Technol.* 51: 39-46.

Behrendt A., de Beer D. & Stief P. 2013. Vertical activity distribution of dissimilatory nitrate reduction in coastal marine sediments. *Biogeosciences Discuss.* 10: 8065-8101.

Behrendt A., Tarre S., Beliavski M., Green M., Klatt J., de Beer D. & Stief P. 2014. Effect of high electron donor supply on dissimilatory nitrate reduction pathways in a bioreactor for nitrate removal. *Bioresource Technol.* 171: 291-297.

Bergström A.-K. & Jansson M. 2006. Atmospheric nitrogen deposition has caused nitrogen enrichment and eutrophication of lakes in the northern hemisphere. *Glob. Change Biol.* 12: 635-643.

Brunet R.C. & Garcia-Gil L.J. 1996. Sulfide-induced dissimilatory nitrate reduction to ammonia in anaerobic freshwater sediments. *FEMS Microbiol. Ecol.* 21: 131-138.

Canfield D.E., Kristensen E. & Thamdrup B. 2005. *Aquatic Geomicrobiology*. Elsevier Academic Press, San Diego, 656 p.

Carrey R., Rodríguez-Escales P., Otero N., Ayora C., Soler A. & Gómez-Alday J.J. 2014. Nitrate attenuation potential of hypersaline lake sediments in central Spain: Flow-through and batch experiments. *J. Contam. Hydrol.* 164: 323-337.

Chen J. & Strous M. 2013. Denitrification and aerobic respiration, hybrid electron transport chains and co-evolution. *BBA Bioenergetics* 1827: 136-144.

Christensen P.B., Rysgaard S., Sloth N.P., Dalsgaard T. & Schwärter S. 2000. Sediment mineralization, nutrient fluxes, denitrification and dissimilatory nitrate reduction to ammonium in an estuarine fjord with sea cage trout farms. *Aquat. Microb. Ecol.* 21: 73–84.

Conley C.J., Pearl H.W., Howarth R.W., Boesch D.F., Seitzinger S.P., Havens K.E., Lancelot C. & Likens G.E. 2009. Controlling eutrophication: nitrogen and phosphorous. *Science* 323: 1014-1015.

Cornwell J.C., Kemp W.M. & Kana T.M. 1999. Denitrification in coastal ecosystems: methods, environmental controls, and ecosystem level controls, a review. *Aquat. Ecol.* 33: 41-54.

Dong L.F., Sobey M.N., Smith C.J., Rusmana I., Phillips W., Stott A., Osborn A.M. & Nedwell D.B. 2011. Dissimilatory reduction of nitrate to ammonium, not denitrification or anammox, dominates benthic nitrate reduction in tropical estuaries. *Limnol. Oceanogr.* 56: 279-291.

Francis C.A. 2012. Personal homepage http://earthsci.stanford.edu/~caf/ Cited 12th June 2014.

Francis C.A., Beman J.M. & Kuypers M.M.M. 2007. New processes and players in the nitrogen cycle: the microbial ecology of anaerobic and archaeal ammonia oxidation. *ISME J.* 1: 19-27.

Fry B. 2006. *Stable Isotope Ecology.* Springer Science+Business Media, New York, 308 p.

Han H., Lu X., Burger D.F., Joshi U.M. & Zhang L. 2014. Nitrogen dynamics at the sediment-water interface in a tropical reservoir. *Ecol. Eng.* 73: 146-153.

Harrison J.A., Maranger R.J., Alexander R.B., Giblin A.E., Jacinthe P.-A., Mayorga E., Seitzinger S. P., Sobota D.J. & Wollheim W.M. 2009. The regional and global significance of nitrogen removal in lakes and reservoirs. *Biogeochemistry* 93: 143-157.

Harrison M.D., Miller A.J., Groffman P.M., Mayer P.M & Kaushal S.S. 2014. Hydrologic controls on nitrogen and phosphorous dynamics in relict Oxbow wetlands adjacent to an urban restored stream. *J. Am. Water Resour. As.* 50: 1365-1382.

Hayes J.M. 2002. *Practice and Principles of Isotopic Measurements in Organic Geochemistry.* Woods Hole Oceanographic Institution, Massachusetts, 25 p.

Herbert R.A. 1999. Nitrogen cycling in marine ecosystems. *FEMS Microbiol. Rev.* 23: 563-590.

Holmroos H., Hietanen S., Niemistö J. & Horppila J. 2012. Sediment resuspension and denitrification affect the nitrogen to phosphorus ratio of shallow lake waters. *Fundam. Appl. Limnol.* 180: 193-205.

Jaeglé L., Steinberger L., Martin R.V. & Chance K. 2005. Global partitioning of NO_x sources using satellite observations: Relative roles of fossil fuel combustion, biomass burning and soil emissions. *Faraday Discuss.* 130: 407-423.

Järviwiki 2014. Keurusselkä - Ukonselkä (yhd.) http://www.jarviwiki.fi/wiki/Keurusselk%C3%A4_-_Ukonselk%C3%A4_%28yhd.%29 Cited 14th January 2014.

Kirchman D.L. 2012. *Processes in Microbial Ecology*. School of Marine Science and Policy, University of Delaware, USA, 328 p.

Kokemäenjoen vesistön vesiensuojeluyhdistys 2011. *Vuosiyhteenveto Jaakonsuon puhdistamon purkuvesistön velvoitetarkkailusta vuodelta 2010.*

Kraft B., Tegetmeyer H.E., Sharma R., Klotz M.G., Ferdelman T.G., Hettich R.L., Geelhoed J.S. & Strous M. 2014. The environmental controls that govern the end product of bacterial nitrate respiration. *Science* 345: 676-679.

Laverman A.M., Canavan R.W., Slomp C.P. & Van Cappellen P. 2007. Potential nitrate removal in a coastal freshwater sediment (Haringvliet Lake, The Netherlands) and response to salinization. *Water Res.* 41: 3061-3068.

Liikanen A., Tanskanen H., Murtoniemi T. & Martikainen P. 2002. A laboratory microcosm for simultaneous gas and nutrient flux measurements in sediments. *Boreal Environ. Res.* 7:151-160.

Maanmittauslaitos 2014. Paikkatietoikkuna. http://www.paikkatietoikkuna.fi/ Cited 14th January 2014.

Marchant H.K., Lavik G., Holtappels M. & Kuypers M.M.M. 2014. The fate of nitrate in intertidal permeable sediments. *PloS One* 9: e104517.

Mazéas L., Vigneron V., Le-Ménach K., Budzinski H., Audic J.M., Bernet N. & Bouchez T. 2008. Elucidation of nitrate reduction pathways in anaerobic bioreactors using a stable isotope approach. *Rapid Commun. Mass Spectrom.* 22: 1746-1750.

McCrackin M.L. & Elser J.J. 2010. Atmospheric nitrogen deposition influences denitrification and nitrous oxide production in lakes. *Ecology* 91: 528-539.

Merchán D., Otero N., Soler A. & Causapé J. 2014. Main sources and processes affecting dissolved sulphates and nitrates in a small irrigated basin (Lerma Basin, Zaragoza, Spain): Isotopic characterization. *Agr. Ecosyst. Environ.* 195: 127-138.

Minjeaud L., Bonin P.C. & Michotey V.D. 2008. Nitrogen fluxes from marine sediments: quantification of the associated co-occurring bacterial processes. *Biogeochemistry* 90: 141-157.

Misiti T.M., Hajaya M.G. & Pavlostathis S.G. 2011. Nitrate reduction in a simulated free-water surface wetland system. *Water Res.* 45: 5587-5598.

Nielsen L.P. 1992. Denitrification in sediment determined from nitrogen isotope pairing. *FEMS Microbiol. Ecol.* 9: 357-361.

Nizzoli D., Carraro E., Nigro V. & Viaroli P. 2010. Effect of organic enrichment and thermal regime on denitrification and dissimilatory nitrate reduction to ammonium (DNRA) in hypolimnetic sediments of two lowland lakes. *Water Res.* 44: 2715-2724.

Ogilvie B.G., Rutter M. & Nedwell D.B. 1997. Selection by temperature of nitrate-reducing bacteria from estuarine sediments: species composition and competition for nitrate. *FEMS Microbiol. Ecol.* 23: 11-22.

OIVA ympäristö- ja paikkatietopalvelu 2014. Keurusselkä. https://wwwp2.ymparisto.fi/scripts/oiva.asp Cited 23rd January 2014.

Pan Y., Ye L., Ni B.-J. & Yuan Z. 2012. Effect of pH on N_2O reduction and accumulation during denitrification by methanol utilizing denitrifiers. *Water Res.* 46: 4832-4840.

Rissanen A.J. 2012. *Nitrogen removal by microbial processes in aquatic systems.* University of Jyväskylä, Finland.

Rissanen A.J., Tiirola M. & Ojala A. 2011. Spatial and temporal variation in denitrification and in the denitrifier community in a boreal lake. *Aquat. Microb. Ecol.* 64: 27-40.

Rissanen A.J., Tiirola M., Hietanen S. & Ojala A. 2013. Interlake variation and environmental controls of denitrification across different geographical scales. *Aquat. Microb. Ecol.* 69: 1-16.

Rysgaard S., Risgaard-Petersen N. & Sloth N.P. 1996. Nitrification, denitrification, and nitrate ammonification in sediments of two coastal lagoons in Southern France. *Hydrobiologia* 329: 133-141.

Schindler D.W. 2006. Recent advances in the understanding and management of eutrophication. *Limnol. Oceanogr.* 51: 356-363.

Scott J.T., McCarthy M.J., Gardner W.S. & Doyle R.D. 2008. Denitrification, dissimilatory nitrate reduction to ammonium, and nitrogen fixation along a nitrate concentration gradient in a created freshwater wetland. *Biogeochemistry* 87: 99-111.

Shapleigh J.P. 2013. Denitrifying Prokaryotes. In: Rosenberg E. (ed.), *The Prokaryotes*, 405-425. Springer, Berlin.

Sigman D.M., Altabet M.A., Michener R., McCorkle D.C., Fry B. & Holmes R.M. 1997. Natural abundance-level measurement of the nitrogen isotopic composition of oceanic nitrate: an adaptation of the ammonia diffusion method. *Mar. Chem.* 57: 227-242.

Simon J. 2002. Enzymology and bioenergetics of respiratory nitrite ammonification. *FEMS Microbiol. Rev.* 26: 285-309.

Song B., Lisa J.A. & Tobias C.R. 2014. Linking DNRA community structure and activity in a shallow lagoonal estuarine system. *Front Microbiol.* 5: 460-470.

Song Z., Zhou X., Li Y., Yang M. & Xing J. 2013. Bio-desulfurization and denitrification by anaerobic-anoxic process for the treatment of wastewater from flue gas washing. *Water Sci. Technol.* 67: 2042-2049.

Steingruber S.M., Friedrich J., Gächter R. & Wehrli B. 2001. Measurement of denitrification in sediments with the ^{15}N isotope pairing technique. *Appl. Environ. Microbiol.* 67: 3771–3778.

Tan C., Ma F. & Qiu S. 2013. Impact of carbon to nitrogen ratio on nitrogen removal at a low oxygen concentration in a sequencing batch biofilm reactor. *Water Sci. Technol.* 67: 612-618.

Tomaszek J.A. & Gruca-Rokosz R. 2007. Rates of dissimilatory nitrate reduction to ammonium in two Polish reservoirs: Impacts of temperature, organic matter content, and nitrate concentration. *Environ. Technol.* 28: 771-778.

Tuominen L., Heinänen A., Kuparinen J. & Nielsen L.P. 1998. Spatial and temporal variability of denitrification in the sediments of the northern Baltic Proper. *Mar. Ecol. Prog. Ser.* 172: 13-24.

Vitousek P., Aber J., Howarth R., Likens G., Matson P., Schindler D., Schlesinger W. & Tilman D. 1997. Human alteration of the global nitrogen cycle: sources and consequences. *Ecol. Appl.* 7: 737-750.

Voss M., Dippner J.W., Humborg C., Hürdler J., Korth F., Neumann T., Schernewski G. & Venohr M. 2011. History and scenarios of future development of Baltic Sea eutrophication. *Estuar. Coast Shelf S.* 92: 307-322.

Warneke S., Schipper L.A., Matiasek M.G., Scow K.M., Cameron S., Bruesewitz D.A. & McDonald I. R. 2011. Nitrate removal, communities of denitrifiers and adverse effects in different carbon substrates for use in denitrification beds. *Water Res.* 45: 5463-5475.

Zhang Y., Zhu H., Yan B., Li X. & Ou Y. 2013. Effects of plant and water level on nitrogen variation in overlying and pore water of agricultural drainage ditches in Sanjiang plain, Northeast China. *CLEAN-Soil Air Water* 42: 386-392.

Zhao Y., Xia Y., Li B. & Yan X. 2014. Influence of environmental factors on net N_2 and N_2O production in sediment of freshwater rivers. *Environ. Sci. Pollut. Res.* 21: 9973-9982.

Zumft W. G. 1997. Cell biology and molecular basis of denitrification. *Microbiol. Mol. Biol. R.* 61: 533-616.

APPENDIX 1

Tests of IPT assumptions from occasions when there were at least four samples available. *D14*: natural denitrification; *D15*: labeled denitrification; *DNRA14*: natural DNRA; *DNRA15*: labeled DNRA.

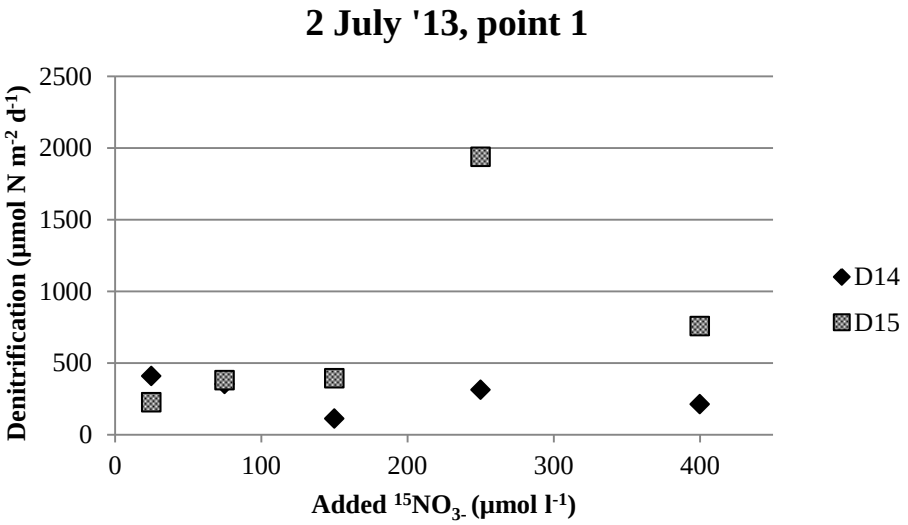

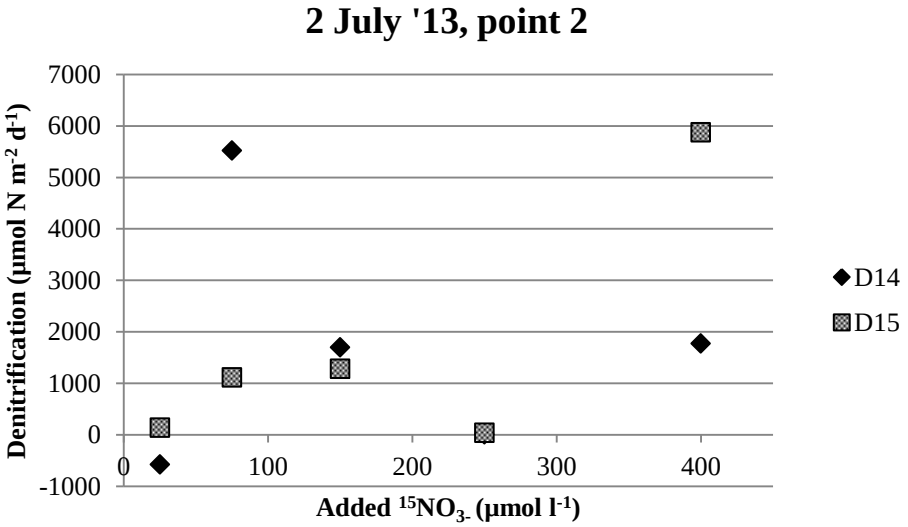

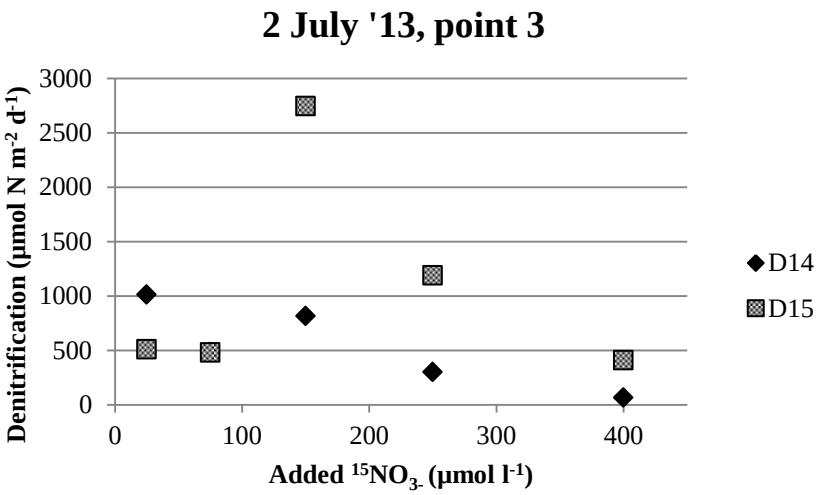
2 July '13, point 3
Denitrification (µmol N m-2 d-1)
3000
2500
2000
1500
1000
500
0
0
100
200
300
400
Added 15NO3- (µmol l-1)
D14
D15

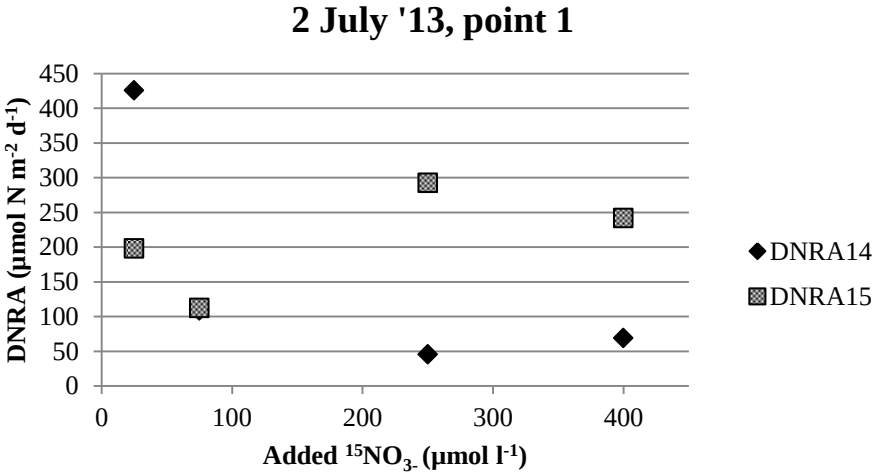
2 July '13, point 1
DNRA (µmol N m-2 d-1)
450
400
350
300
250
200
150
100
50
0
0
100
200
300
400
Added 15NO3- (µmol l-1)
DNRA14
DNRA15

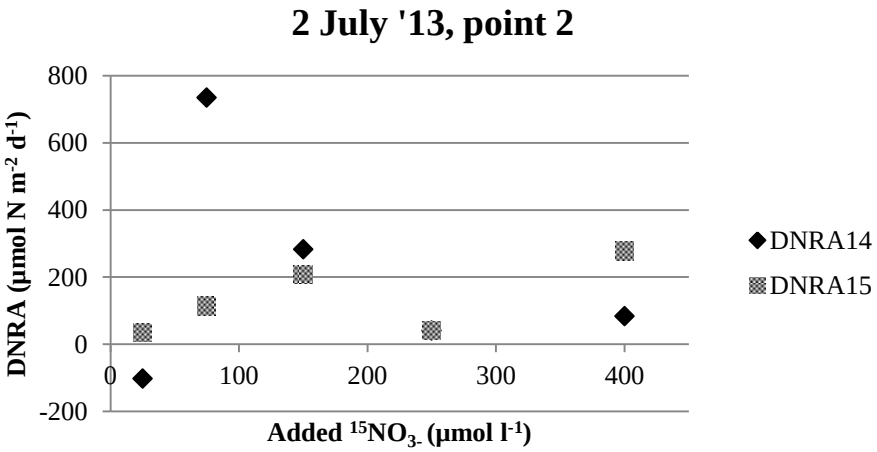
2 July '13, point 2
DNRA (µmol N m-2 d-1)
800
600
400
200
0
-200
0
100
200
300
400
Added 15NO3- (µmol l-1)
DNRA14
DNRA15

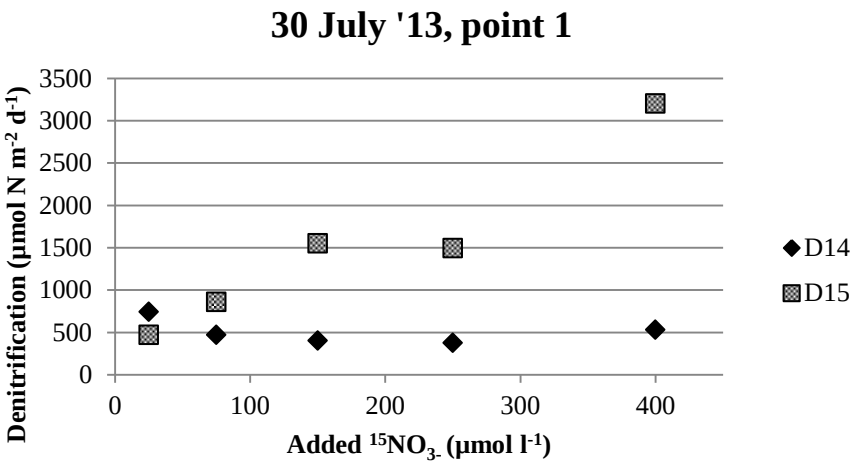
30 July '13, point 1
Denitrification (µmol N m-2 d-1)
3500
3000
2500
2000
1500
1000
500
0
0
100
200
300
400
Added 15NO3- (µmol l-1)
D14
D15

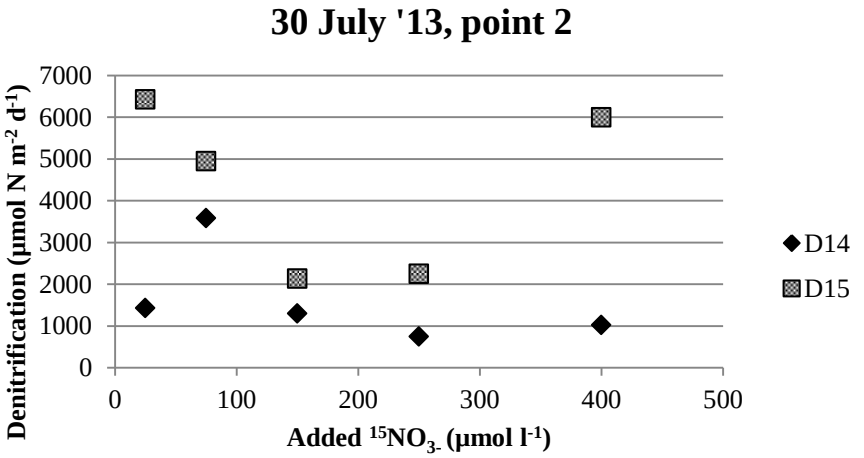
30 July '13, point 2
Denitrification (µmol N m-2 d-1)
7000
6000
5000
4000
3000
2000
1000
0
0
100
200
300
400
500
Added 15NO3- (µmol l-1)
D14
D15

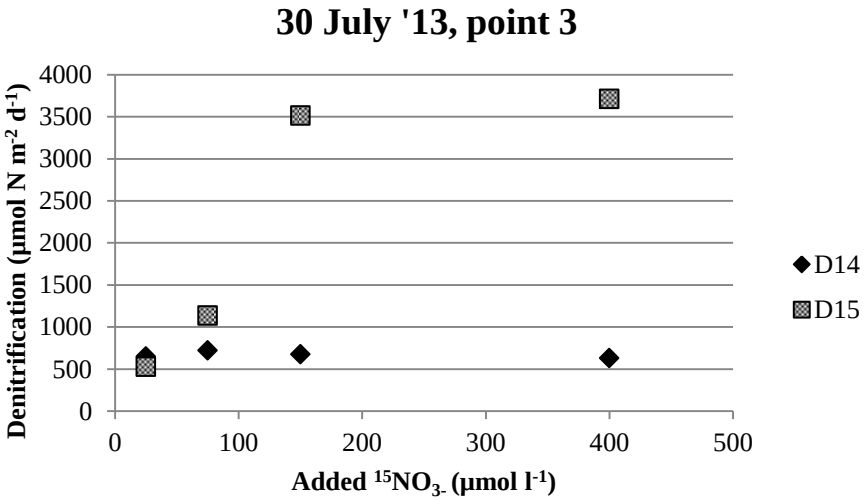
30 July '13, point 3
Denitrification (µmol N m-2 d-1)
4000
3500
3000
2500
2000
1500
1000
500
0
0
100
200
300
400
500
Added 15NO3- (µmol l-1)
D14
D15

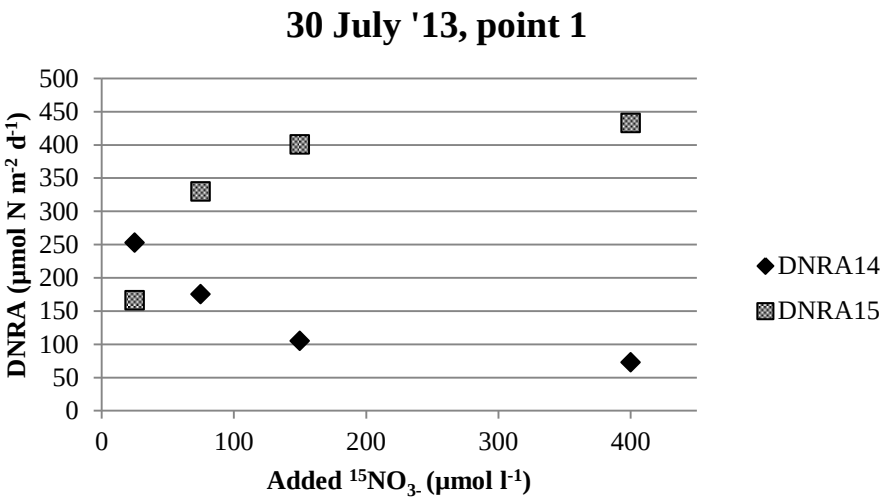
30 July '13, point 1
DNRA (µmol N m-2 d-1)
500
450
400
350
300
250
200
150
100
50
0
0
100
200
300
400
Added 15NO3- (µmol l-1)
DNRA14
DNRA15

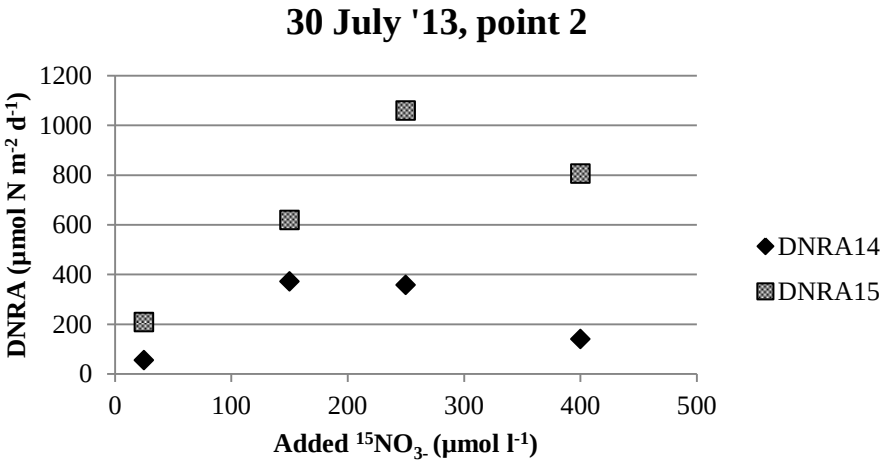
30 July '13, point 2
DNRA (µmol N m-2 d-1)
1200
1000
800
600
400
200
0
0
100
200
300
400
500
Added 15NO3- (µmol l-1)
DNRA14
DNRA15

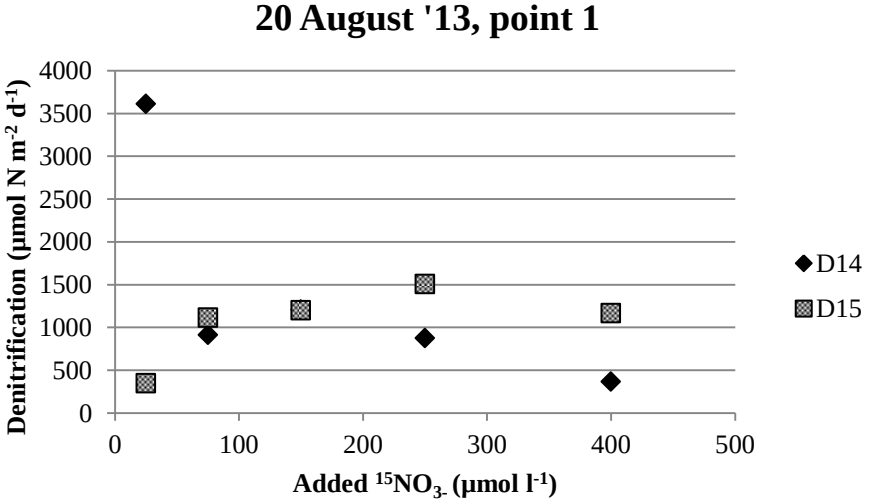
20 August '13, point 1
Denitrification (µmol N m-2 d-1)
4000
3500
3000
2500
2000
1500
1000
500
0
0
100
200
300
400
500
Added 15NO3- (µmol l-1)
D14
D15

20 August, point 3

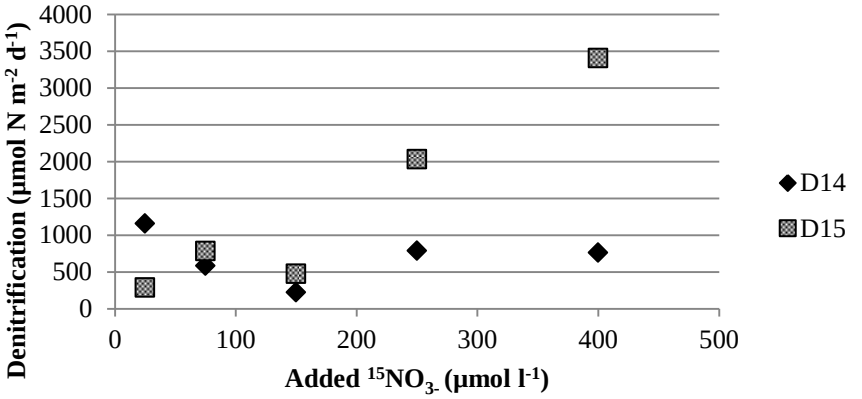

20 August '13, point 1

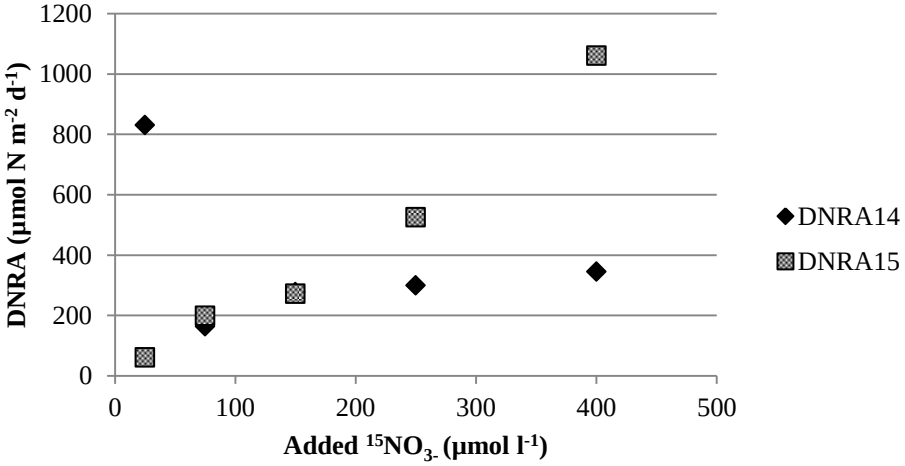

20 August '13, point 3

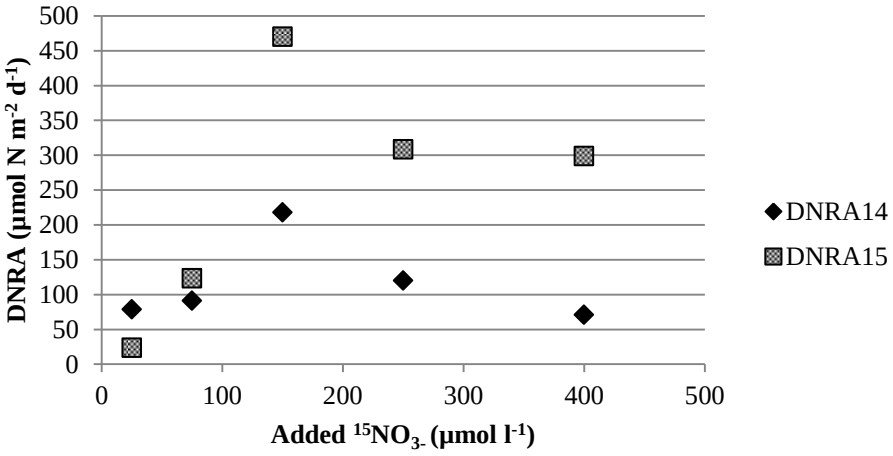

12 November '13, point 1

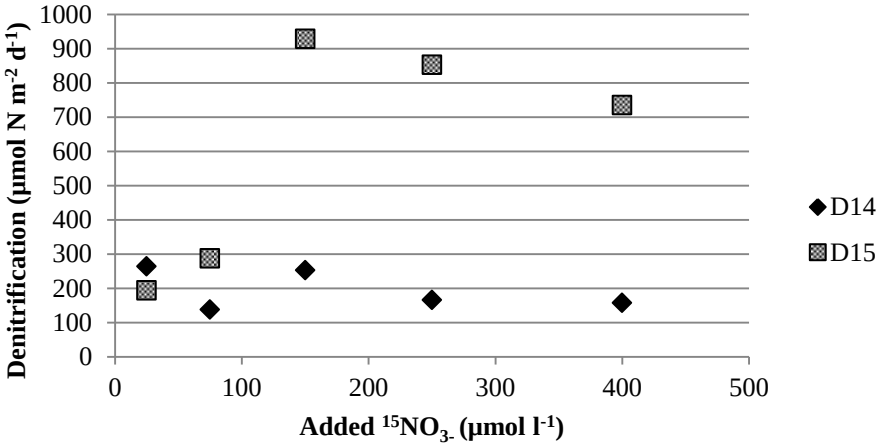

12 November '13, point 2

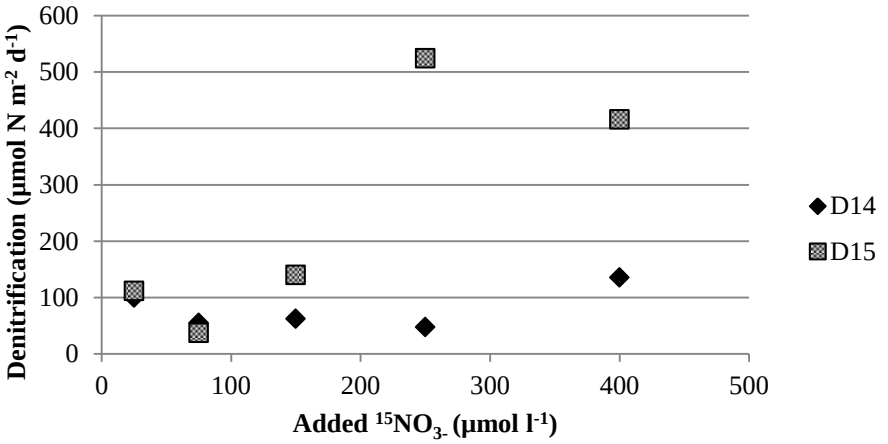

12 November '13, point 3

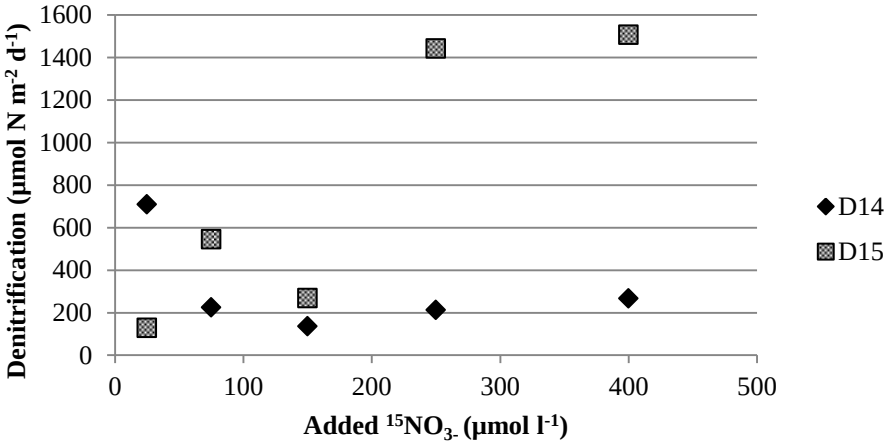

12 November '13, point 1

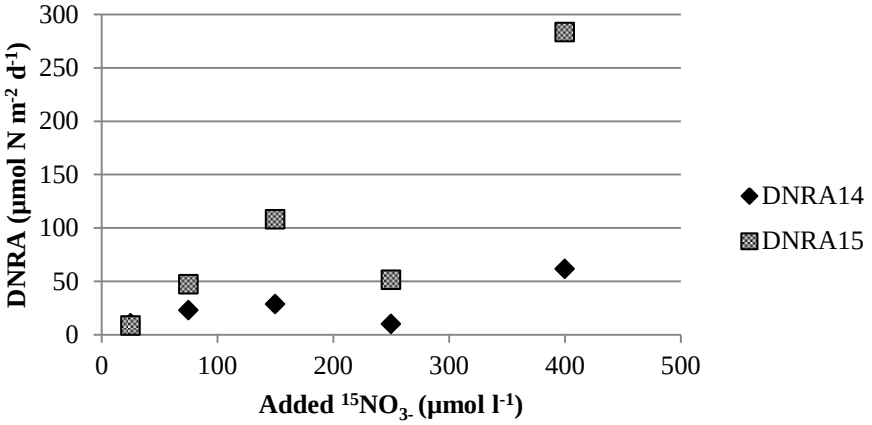

12 November '13, point 2

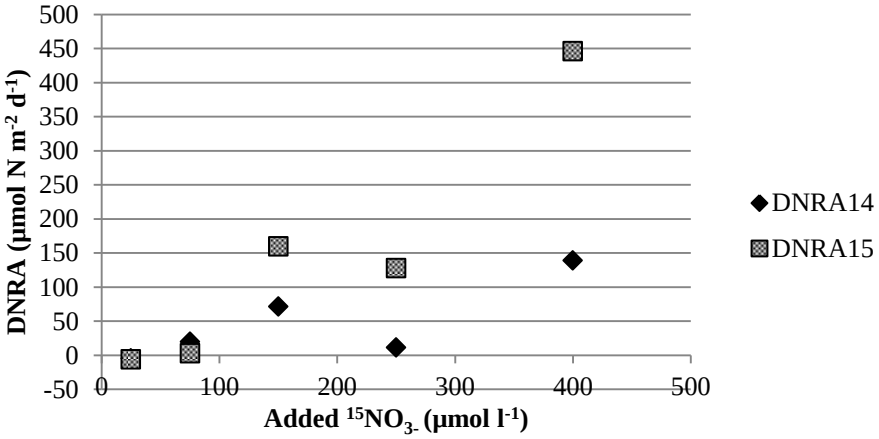

12 November '13, point 3

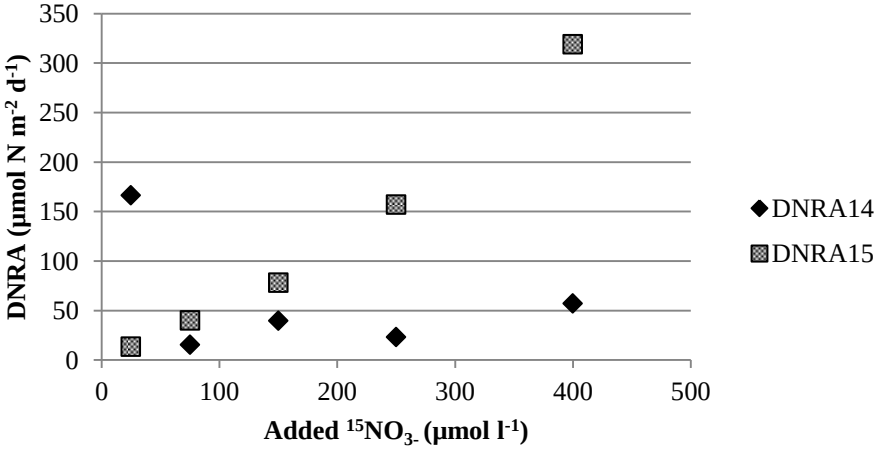

10 February '14, point 1

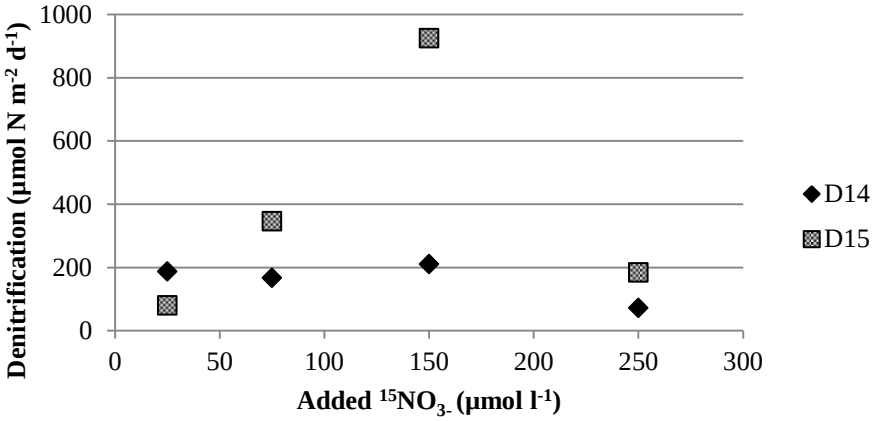

10 February '14, point 2

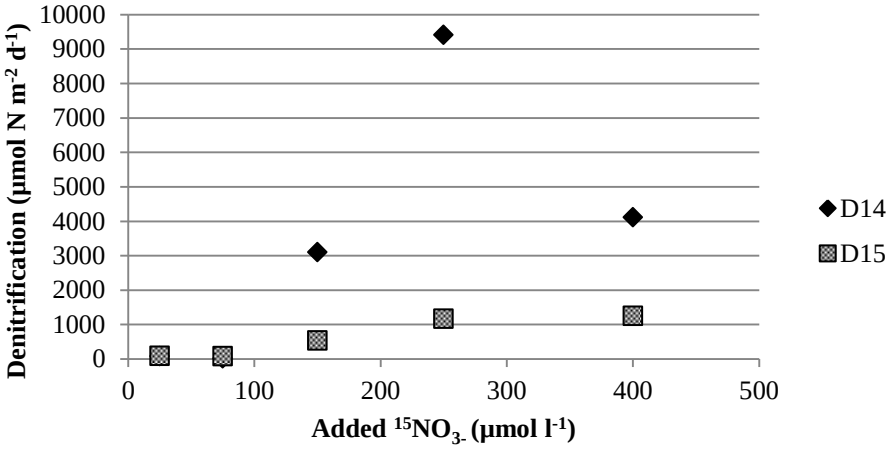

10 February '14, point 3

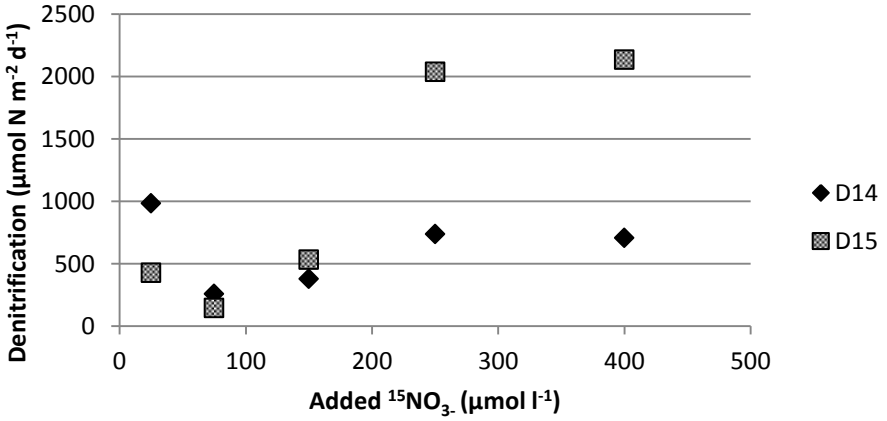

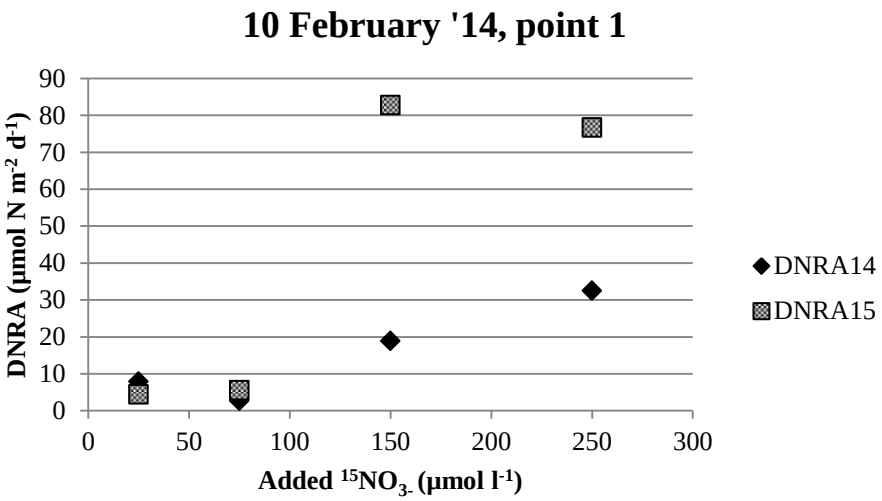
10 February '14, point 1
DNRA (µmol N m-2 d-1)
90
80
70
60
50
40
30
20
10
0
0
50
100
150
200
250
300
Added 15NO3- (µmol l-1)
DNRA14
DNRA15

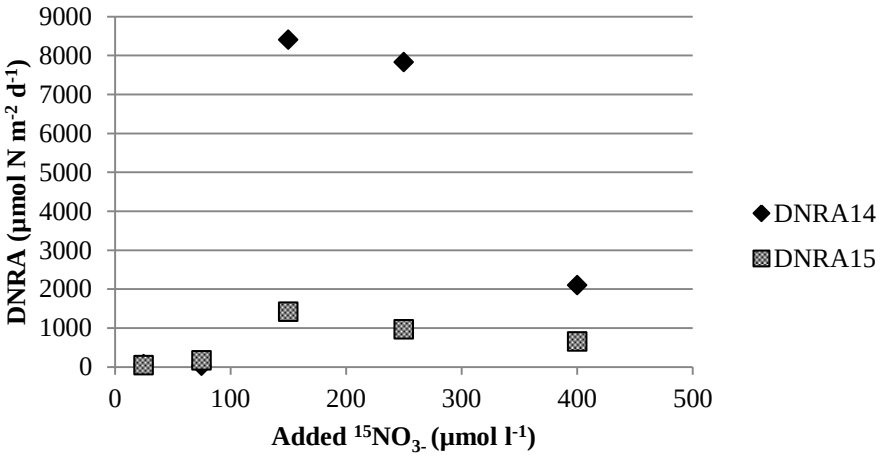
10 February '14, point 2
DNRA (µmol N m-2 d-1)
9000
8000
7000
6000
5000
4000
3000
2000
1000
0
0
100
200
300
400
500
Added 15NO3- (µmol l-1)
DNRA14
DNRA15